
Retrieval Augmented Reinforcement Learning

Anirudh Goyal¹ Abram L. Friesen^{*2} Theophane Weber^{*2} Andrea Banino^{*2} Nan Rosemary Ke^{*2}
Adria Puigdomenech Badia² Arthur Guez² Mehdi Mirza² Peter C. Humphreys² Ksenia Konyushkova²
Laurent Sifre² Michal Valko² Simon Osindero² Timothy Lillicrap² Nicolas Heess² Charles Blundell²

Abstract

Most deep reinforcement learning (RL) algorithms distill experience into parametric behavior policies or value functions via gradient updates. While effective, this approach has several disadvantages: (1) it is computationally expensive, (2) it can take many updates to integrate experiences into the parametric model, (3) experiences that are not fully integrated do not appropriately influence the agent’s behavior, and (4) behavior is limited by the capacity of the model. In this paper we explore an alternative paradigm in which we train a network to map a dataset of past experiences to optimal behavior. Specifically, we augment an RL agent with a retrieval process (parameterized as a neural network) that has direct access to a dataset of experiences. This dataset can come from the agent’s past experiences, expert demonstrations, or any other relevant source. The retrieval process is trained to retrieve information from the dataset that may be useful in the current context, to help the agent achieve its goal faster and more efficiently. The proposed method facilitates learning agents that at test-time can condition their behavior on the entire dataset and not only the current state, or current trajectory. We integrate our method into two different RL agents: an offline DQN agent and an online R2D2 agent. In offline multi-task problems, we show that the retrieval-augmented DQN agent avoids task interference and learns faster than the baseline DQN agent. On Atari, we show that retrieval-augmented R2D2 learns significantly faster than the baseline R2D2 agent and achieves higher scores. We run extensive ablations to measure the contributions of the components of our proposed method.

^{*}Equal contribution ¹Mila, Université de Montréal
²DeepMind. Correspondence to: Anirudh Goyal <anirudhgoyal9119@gmail.com>.

1. Introduction

A host is preparing a holiday meal for friends. They remember that the last time they went to the grocery store during the holiday season, all of the fresh produce was sold out. Thinking back to this past experience, they decide to go early! The hypothetical host is employing *case-based reasoning* (e.g., Kolodner, 1992; Leake, 1996). Here, an agent *recalls* a situation similar to the current one and uses information from the previous experience to solve the current task. This may involve adapting old solutions to meet new demands, or using previous experiences to make sense of new situations.

In contrast, a dominant paradigm in modern reinforcement learning (RL) is to learn general purpose behaviour rules from the agent’s past experience. These rules are typically represented in the weights of a parametric policy or value function network model. Most deep RL algorithms integrate information *across trajectories* by iteratively updating network parameters using gradients that are computed along *individual trajectories* (collected online or stored in an experience replay dataset, Lin, 1992). For example, many off-policy algorithms reuse past experience by “replaying” trajectory snippets in order to compute weight updates for a value function represented by a deep network (Ernst et al., 2005; Riedmiller, 2005; Mnih et al., 2015b; Heess et al., 2015; Lillicrap et al., 2015).

This paradigm has clear advantages but at least two inter-related limitations: First, after learning, an agent’s past experiences no longer play a direct role in the agent’s behavior, even if they are relevant to the current situation. This occurs because detailed information in the agent’s past experience is lost due to practical constraints on network capacity. Second, since the information provided by individual trajectories first needs to be distilled into a general purpose parametric rule, an agent may not be able to exploit the specific guidance that a handful of individual past experiences could provide, nor rapidly incorporate novel experience that becomes available—it may take many replays through related traces in the past experiences for this to occur (Weisz et al., 2021).

In this work, we develop an algorithm that overcomes these

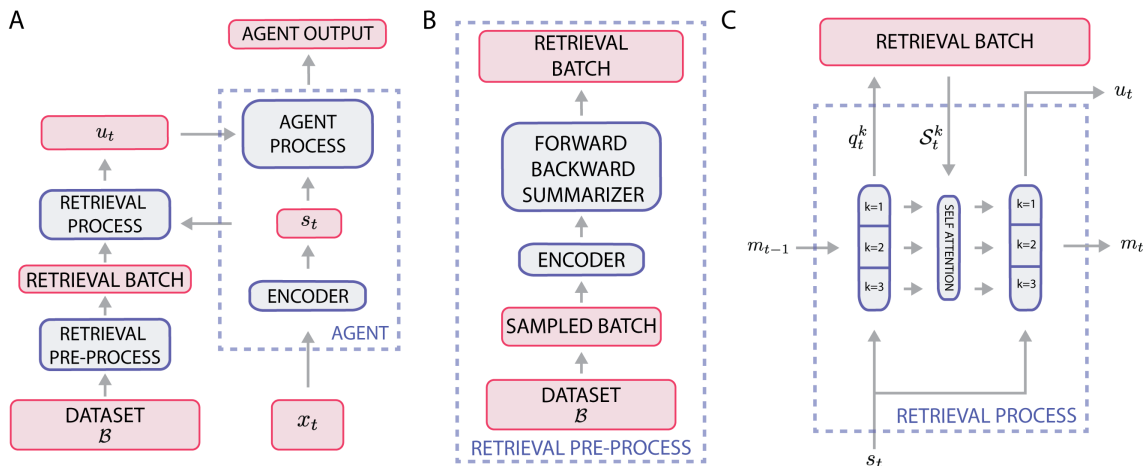


Figure 1: **Retrieval-augmented agent (R2A) architecture:** (A) R2A augments the agent with a retrieval process. The retrieval process and the agent maintain separate internal states, m_t and s_t , respectively. The retrieval process retrieves information relevant to the agent’s current internal state s_t from the retrieval batch, which is a pre-processed sample from the retrieval dataset \mathcal{B} . The retrieved information u_t is used by the agent process to inform its output (e.g., a policy or value function). (B) A batch of raw trajectories is sampled from the retrieval dataset \mathcal{B} and encoded (using the same encoder as the agent). Each encoded trajectory is then summarized via forward and a backward summarization functions (section 2.2) and sent to the retrieval process. (C) The retrieval process is parameterized as a recurrent model and the internal state m_t is partitioned into slots. Each slot independently retrieves information from the retrieval batch, which is used to update the slot’s representation and sent to the agent process in u_t . Slots also interact with each other via self-attention. See section 2.3 for more details.

limitations by *augmenting* a standard reinforcement learning agent with a *retrieval process* (parameterized via a neural network). The purpose of the retrieval process is to help the agent achieve its objective by providing relevant contextual information. To this end, the retrieval process uses a learned attention mechanism to dynamically access a large pool of past trajectories stored in a dataset (e.g., a replay buffer), with the aim of integrating information across these. The proposed algorithm (R2A), shown in Figure 1, enables an agent to retrieve information from a dataset of trajectories. The high-level idea is to have two different processes. First, the *retrieval process* makes a “query” for relevant contextual information in the dataset. Second, the *agent process* performs inference and learning based on the information provided by the retrieval process. These two processes have different internal states but interact to shape the representations and predictions of each other: the agent process provides the relevant context, and the retrieval process uses the context and its own internal state to generate a query and retrieve relevant information, which is in turn used by the agent process to shape the representation of its policy and value function (see Fig. 1A). Our proposed retrieval-augmented RL paradigm could take several forms. Here, we focus on one particular instantiation applied to multiple different RL agents and environments to validate our hypothesis that learning a retrieval process can help an RL agent achieve its objective.

Summary of experimental results. We first show that the performance and sample efficiency of R2D2 (Kapturowski et al., 2018), a state-of-the-art off-policy RL algorithm, on Atari games can be improved by retrieval augmentation. In this setting, we run a series of ablations to

demonstrate the benefits of our design decisions and to show how our approach compares with related work. In online Atari, the agent retrieves from its own experiences on the same game; however, retrieval can also query external data from other agents or other tasks. We thus evaluated on three separate multi-task offline RL environments (gridroboman, BabyAI (Chevalier-Boisvert et al., 2018), CausalWorld (Ahmed et al., 2020) (a continuous control benchmark), where the retrieved data is first from a different agent in the same task and then from different agents and includes data from other tasks. In all cases, the retrieval-augmented agent learns faster and achieves higher reward.

2. Retrieval-Augmented Agents

We now present our method for augmenting an RL agent with a retrieval process, thereby reducing the agent’s dependence on its model capacity, and enabling fast and flexible use of past experiences. A retrieval-augmented agent (R2A) consists of two main components: (1) the retrieval process, which takes in the current state of the agent, combines this with its own internal state, and retrieves relevant information from an external dataset of experiences; and (2) a standard reward-maximizing RL agent, which uses the retrieved information to improve its value or policy estimates. See Figure 1 for an overview. The retrieval process is trained to retrieve information that the agent can use to improve its performance, without explicit knowledge of the agent’s policy. Importantly, the retrieval process has its own internal state, which enables it to integrate and combine information across retrievals. In the following, we focus on value-based methods, such as DQN (Mnih et al., 2015a) and R2D2 (Kapturowski et al., 2018), but our approach is equally applicable

to policy-based methods.

2.1. Retrieval-augmented agent

Formally, the agent receives an input x_t at each timestep t . Each input is processed by a neural encoder (e.g., a resnet if the input is an image) to obtain an abstract internal state for the agent $s_t = f_{\theta}^{\text{enc}}(x_t)$. For clarity, we focus here on the case of a single vector input, however, each input could also include the history of past observations, actions, and rewards, as is the case when f_{θ}^{enc} is a recurrent network. These embeddings are used by the agent and retrieval processes. The retrieval process operates on a dataset $\mathcal{B} = \{((x_t, a_t, r_t), \dots, (x_{t+l}, a_{t+l}, r_{t+l}))\}$ of l -step trajectories, for $l \geq 1$. This dataset could come from other agents or experts, as in offline RL or imitation learning, or consist of the growing set of the agent’s own experiences. Then, a retrieval-augmented agent (R2A) consists of the retrieval process and the agent process, parameterized by $\theta = \{\theta^{\text{enc}}, \theta^{\text{retr}}, \theta^{\text{agent}}\}$,

$$\begin{aligned} \text{Retrieval process } f_{\theta, \mathcal{B}}^{\text{retr}} : m_{t-1}, s_t &\mapsto m_t, u_t \\ \text{Agent process } f_{\theta}^{\text{agent}} : s_t, u_t &\mapsto Q_{\theta}(s_t, u_t, a) \end{aligned}$$

Retrieval Process. The retrieval process is parameterized as a neural network and has an internal state m_t . The retrieval process takes in the current abstract state of the agent process s_t and its own previous internal state m_{t-1} and uses these to retrieve relevant information from the dataset \mathcal{B} , which it then summarizes in a vector u_t , and also updates its internal state m_t .

Agent Process. The state of the agent s_t and the information from the retrieval process u_t are then passed to the action-value function, itself used to select external actions.

The above defines a parameterization for a retrieval-augmented agent. For retrieval to be effective, the retrieval process needs to: (1) be able to efficiently query a large dataset of trajectories, (2) learn and employ a similarity function to find relevant trajectories, and (3) encode and summarize the trajectories in a manner that allows efficient discovery of relevant past and future information.

Below, we explain how we achieve these desiderata. At a high-level, to reduce computational complexity given a experience dataset of hundreds of thousands of trajectories, R2A operates on samples from the dataset. R2A then encodes and summarizes the sampled trajectories using auxiliary losses and bi-directional sequence models to enable efficient retrieval of temporal information. Finally, R2A uses attention to select semantically relevant trajectories.

2.2. Retrieval batch sampling and pre-processing.

Sampling a retrieval batch from the retrieval dataset. To reduce computational complexity, R2A uniformly samples a large batch of past experiences from the retrieval dataset

and then retrieves from the sampled batch. We denote the sampled batch as the “retrieval batch” and the number of trajectories in the retrieval batch as $n_{\text{retrieval}}$.

Encoding and forward-backward summarization of the retrieval dataset and corresponding auxiliary losses. Since the agent’s internal state extracts information from observations which relate to the task at hand, we choose to re-encode the raw experiences in the “retrieval batch” using the agent encoder module (i.e., f_{θ}^{enc}). However, this representation is a function only of past observations (i.e., it’s a causal representation) and may not be fully compatible with the needs of the retrieval operation. For that reason, we propose to further encode the retrieved batch of information by a learned *summarization* function, applied on the output of the encoder module, which captures information about the past and the future within a particular trajectory by using a bi-directional model (e.g., parameterized as a bi-directional RNN or a transformer).

$$\begin{aligned} \text{Forward Summarizer } f_{\theta}^{\text{fwd}} : (s_1, \dots, s_t) &\mapsto h_t \\ \text{Backward Summarizer } f_{\theta}^{\text{bwd}} : (s_l, \dots, s_t) &\mapsto b_t \end{aligned}$$

For each trajectory in the retrieval batch, we represent each time-step within a trajectory by a set of two vectors $h_{i,t}$ and $b_{i,t}$ (Figure 5 in the appendix) where $h_{i,t}$ summarizes the past (i.e., from $t' = 0$ to $t' = t$ time-steps of the i^{th} trajectory) while $b_{i,t}$ summarizes the future (i.e., from $t' = t$ to $t' = l$ time-steps) within the i^{th} trajectory. In addition, taking inspiration from (Jaderberg et al., 2016; Ke et al., 2019; Devlin et al., 2018; Mazouze et al., 2020), we use auxiliary losses to improve modeling of long term dependencies when training the parameters of our forward and backward summarizers. The goal of these losses is to force the representation $(h_{i,t}, b_{i,t})_{i,t \geq 0}$ to capture meaningful information for the unknown downstream task. For our experiments, we use supervised losses where we have access to actions or rewards in the retrieval batch. For ablations we also experiment with self-supervised losses. For supervised auxiliary losses, we use policy, value, and reward prediction (Silver et al., 2017; Schrittwieser et al., 2019), and for self-supervised losses, we use a BERT-style masking loss (Devlin et al., 2018).

2.3. Retrieving contextual information.

In this section, we explain how the retrieval process, when provided with relevant contextual information represented by the agent’s current state s_t , interacts with the summarized information in the retrieval batch to select information u_t to provide to the agent in return.

Retrieval process state parameterization. We parameterize the process that retrieves information from past experience as a structured parametric model with multiple separate memory slots (or sub-units). The state of the

Algorithm 1 One timestep of a retrieval-augmented agent (R2A).

Input: Current input \mathbf{x}_t , previous retrieval process state $\mathbf{m}_{t-1} = \{\mathbf{m}_{t-1,k} | k \in \{1, \dots, n_f\}\}$, dataset of l -step trajectories $\mathcal{B} = \{((\mathbf{x}_t^i, \mathbf{h}_t^i, \mathbf{b}_t^i, \mathbf{a}_t^i, r_t^i), \dots, (\mathbf{x}_{t+l}^i, \mathbf{h}_{t+l}^i, \mathbf{b}_{t+l}^i, \mathbf{a}_{t+l}^i, r_{t+l}^i))\}$ for $l \geq 1$ and $1 \leq i \leq n_{\text{traj}}$, where \mathbf{h} and \mathbf{b} are the outputs of the forward & backward summarizers. We first encode the current input at time-step t using the encoder $\mathbf{s}_t = f_{\theta}^{\text{enc}}(\mathbf{x}_t)$.

Step 1: Compute the query. For all $1 \leq k \leq n_f$, compute

$$\begin{aligned} \widehat{\mathbf{m}}_{t-1}^k &= \text{GRU}_{\theta}(\mathbf{s}_t, \mathbf{m}_{t-1}^k) \\ \mathbf{q}_t^k &= f_{\text{query}}(\widehat{\mathbf{m}}_{t-1}^k) \end{aligned}$$

Step 2: Identify the most relevant trajectories. For all $1 \leq k \leq n_f, 1 \leq j \leq l$ and $1 \leq i \leq n_{\text{traj}}$,

$$\boldsymbol{\kappa}_{i,j} = (\mathbf{h}_j^i \mathbf{W}_{\text{ret}}^e)^{\text{T}}$$

$$\ell_{i,j}^k = \left(\frac{\mathbf{q}_t^k \boldsymbol{\kappa}_{i,j}}{\sqrt{d_e}} \right)$$

$$\alpha_{i,j}^k = \text{softmax}(\ell_{i,j}^k).$$

Given scores α , the top- k_{traj} trajectories (resp. top- k_{states} states) are selected and denoted by \mathcal{T}_t^k (resp. \mathcal{S}_t^k).

Step 3: Retrieve information from the most relevant trajectories and states.

$$\alpha_{i,j}^k = \text{softmax}(\ell_{i,j}^k), i \in \mathcal{T}_t^k, j \in \mathcal{S}_t^k.$$

$$\mathbf{g}_t^k = \sum_{i,j} \alpha_{i,j}^k \mathbf{v}_{i,j} \text{ where } \mathbf{v}_{i,j} = \mathbf{b}_{i,j} \mathbf{W}_{\text{ret}}^v$$

Step 4: Regularize the retrieved information by using information bottleneck.

$$\mathbf{z}_t^k \sim p(\mathbf{z} | \mathbf{g}_t^k)$$

Step 5: Update the states of the slots.

Slotwise update using retrieved information:

$$\widehat{\mathbf{m}}_t^k \leftarrow \widehat{\mathbf{m}}_{t-1}^k + \mathbf{z}_t^k \quad \forall k \in \{1, \dots, n_f\}$$

Joint slot update through self-attention:

$$\mathbf{c}_t^k = \widehat{\mathbf{m}}_{t-1}^k \mathbf{W}_{\text{SA}}^q \quad \forall k \in \{1, \dots, n_f\}$$

$$\beta_{k,k'} = \text{softmax}_{k'} \left(\frac{\mathbf{c}_t^k \boldsymbol{\kappa}_t^{k'}}{\sqrt{d_e}} \right) \text{ where } \boldsymbol{\kappa}_t^{k'} = (\widehat{\mathbf{m}}_t^{k'} \mathbf{W}_{\text{SA}}^e)^{\text{T}} \quad \forall k, k' \in \{1, \dots, n_f\}$$

$$\mathbf{m}_t^k \leftarrow \widehat{\mathbf{m}}_t^k + \sum_{k'} \beta_{k,k'} \mathbf{v}_{k'} \text{ where } \mathbf{v}_{k'} = \widehat{\mathbf{m}}_t^{k'} \mathbf{W}_{\text{SA}}^v \quad \forall k \in \{1, \dots, n_f\}$$

Step 6: Update the agent state using the retrieved information.

$$\mathbf{d}_t = \mathbf{s}_t \mathbf{W}_{\text{ag}}^q$$

$$\boldsymbol{\kappa}^k = (\mathbf{z}_t^k \mathbf{W}_{\text{ag}}^e)^{\text{T}} \quad \forall k \in \{1, \dots, n_f\}$$

$$\gamma_k = \text{softmax}_k \left(\frac{\mathbf{d}_t \boldsymbol{\kappa}^k}{\sqrt{d_e}} \right)$$

$$\mathbf{u}_t \leftarrow \sum_k \gamma_k \mathbf{v}_k \text{ where } \mathbf{v}_k = \mathbf{z}_t^k \mathbf{W}_{\text{ag}}^v \quad \forall k \in \{1, \dots, n_f\}.$$

$$\mathbf{s}_t \leftarrow \mathbf{s}_t + \mathbf{u}_t$$

retrieval process is a set of n_f memory slots denoted by $\mathbf{m}_t = \{\mathbf{m}_t^k | k \in \{1, \dots, n_f\}\}$ (indexed by the agent time-step t). Slots are initialized randomly at the beginning of the episode. Each slot independently queries and retrieves relevant information from the pool of data. The slots then update their values independently based on the retrieved information, followed by an integration step during which information is shared between slots. Algorithm 1 specifies the six steps of R2A, which we explain in detail below.

Step 1: Query computation. Each slot independently computes its prestate using a GRU on the contextual information from the agent: $\widehat{\mathbf{m}}_{t-1}^k = \text{GRU}_{\theta}(\mathbf{s}_t, \mathbf{m}_{t-1}^k) \quad \forall k \in \{1, \dots, n_f\}$. Then, each slot independently computes a *retrieval query* which will be matched against information in the retrieval batch: $\mathbf{q}_t^k = f_{\text{query}}(\widehat{\mathbf{m}}_{t-1}^k) | k \in \{1, \dots, n_f\}$ ¹

¹ f_{query} is parameterized as a neural network.

where \mathbf{q}_t^k is the query generated by the k^{th} slot at timestep t .

Step 2: Identification of most relevant trajectories and states for each slot (Figure 4A). The retrieval mechanism process uses an attention mechanism to match a query produced by the retrieval state associated with each slot \mathbf{m}_t^k to keys computed on each time step of each trajectory of the retrieval batch. Formally, for each time step and each trajectory in the buffer, we compute a key $\boldsymbol{\kappa}_{i,j}$ by using a linear projection with matrix $\mathbf{W}_{\text{ret}}^e$ on the forward summaries h : $\boldsymbol{\kappa}_{i,j} = (\mathbf{h}_j^i \mathbf{W}_{\text{ret}}^e)^{\text{T}}$. Each query \mathbf{q}_t^k is then matched with the set of all keys $\boldsymbol{\kappa}_{i,j}$, forming attention logits² $\ell_{i,j}^k = \left(\frac{\mathbf{q}_t^k \boldsymbol{\kappa}_{i,j}}{\sqrt{d_e}} \right)$ and corresponding attention weights $\alpha_{i,j}^k = \text{softmax}(\ell_{i,j}^k)$ for $i \leq n_{\text{traj}}, 0 \leq j \leq T$.

²We drop time indexing from attention-related quantities to simplify notation.

Intuitively, $\alpha_{i,j}^k$ captures the extent to which the j^{th} timestep of the i^{th} trajectory in the buffer will be relevant to memory m_t^k through the query q_t^k . It follows that $\sum_j \alpha_{i,j}^k$ is a measure of how relevant the i^{th} trajectory is as a whole for q_t^k . Following previous work (Ke et al., 2018; Goyal et al., 2019b), matching only on the most relevant trajectories will increase the robustness of the retrieval mechanism. We therefore select, for each query, the set \mathcal{T}_t^k of k_{traj} trajectories with highest aggregated score $\sum_j \alpha_{i,j}^k$. Note that typically the queries corresponding to different slots will select different top- k_{traj} trajectories from the retrieval batch. Following the selection of relevant trajectories, we renormalize the weights α , and use another top- k mechanism, this time to choose the set of most relevant states \mathcal{S}_t^k (i.e. which maximizes $\sum_{i \in \mathcal{T}_t^k} \alpha_{i,j}$).

Step 3: Information retrieval from the most relevant trajectories and states (Figure 4B). The next step of the retrieval mechanism consists in computing the renormalized weights α on the subsets \mathcal{T}_t^k and \mathcal{S}_t^k ($\alpha_{i,j}^k = \text{softmax}(\ell_{i,j}^k)$, $i \in \mathcal{T}_t^k$, $j \in \mathcal{S}_t^k$) and using those weights to compute the final retrieved information. The value retrieved from the buffer for query q_t^k is computed as the α -weighted average of a linear function of the *backward* state summaries: $g_t^k = \sum_{i,j} \alpha_{i,j}^k v_{i,j}$ where $v_{i,j} = \mathbf{b}_{i,j} \mathbf{W}_{\text{ret}}^v$.

Step 4: Regularization of the retrieved information via an information bottleneck. We regularize the retrieved information g_t^k via the use of an information bottleneck (Tishby et al., 2000; Alemi et al., 2016). Intuitively, each query pays a price to exploit information from the retrieval batch. Formally, we parametrize two Gaussian distributions $p(Z|g_t^k)$ (which has access to the retrieved information) and $r(Z|m_{t-1})$ (which only has access to the memory units). We define z_t^k as a single sample from $p(Z|g_t^k)$ via the reparameterization trick to ensure differentiability (Kingma & Welling, 2013; Rezende et al., 2014), and ensure that z_t^k does not contain too much information by adding an additional loss $D_{\text{KL}}(p||r)$ to the overall agent loss. We provide more details in the appendix.

Step 5: Slot update. The representation of each slot is first additively updated as a function of the retrieved information $\tilde{m}_t^k \leftarrow \tilde{m}_{t-1}^k + z_t^k$. The final update m_t^k consists of an update in which all slots interact through self-attention (as normally done in transformers; see Algorithm 1 for details).

Step 6: Updating the agent state using retrieved information. The primary goal of the retrieval process is to extract information which may be useful for the agent process. Here, we use the retrieved information to change the state of the agent s_t . In the previous step, the retrieved information is used to change the state of the slots. For this step, we use a similar attention mechanism. Here, the query is a function of the state of the agent process $d_t = s_t \mathbf{W}_{\text{ag}}^q$,

which are matched with the keys $\kappa^k = (z_t^k \mathbf{W}_{\text{ag}}^e)^T \quad \forall k \in \{1, \dots, n_f\}$, as a result of retrieving information, forming attention weights $\gamma_k = \text{softmax}\left(\frac{d_t \kappa^k}{\sqrt{d_e}}\right)$. The values generated as a result of retrieved information by different slots and the attention weights are then used to update the state of the learning agent: $u_t \leftarrow \sum_k \gamma_k v_k$ where $v_k = z_t^k \mathbf{W}_{\text{ag}}^v \quad \forall k \in \{1, \dots, n_f\}$. u_t is the result of the attention over the retrieved information which is then used to change the representation of the agent process: $\tilde{s}_t \leftarrow s_t + u_t$. We also shape the representation of the action-value function $Q(s_t, z_t^k, a_t)$ by conditioning the value function on the retrieved information z_t^k (again via a similar attention mechanism).

3. Experimental Results

To evaluate R2A, we analyze its performance in three different settings. First, to test whether an agent equipped with retrieval augmentation can achieve better performance (i.e., higher rewards) and scale with more, we test the proposed method on the Atari arcade learning environment (ALE) (Bellemare et al., 2013), a single-task off-policy setting where the retrieval process extracts relevant information from the agent’s current replay buffer. We then run a series of ablations of R2A to better understand the roles and effects of its components. Second, to test whether an agent equipped with retrieval augmentation can compensate for lack in capacity when training a single agent on multiple tasks, we evaluate on a multi-task, offline environment that we created, called *gridroboman*. In this environment, a single network is trained on data from all tasks and then, at evaluation time, the retrieval process queries a retrieval dataset containing only data from the task being evaluated. Third, to test if the retrieval augmentation can also benefit when data from the other tasks is present in the retrieval dataset, we evaluate R2A in a multi-task offline version of the BabyAI environment (Chevalier-Boisvert et al., 2018), and a continuous control manipulation benchmark (Ahmed et al., 2020). Again, a single network is trained on all tasks but now the retrieval process queries a retrieval dataset containing data from all tasks.

In our experiments, the retrieval process selects the top $k_{\text{traj}} = 10$ most relevant trajectories (step 2, section 2.3), and then retrieves relevant information from the selected trajectories (step 3, section 2.3) using the top $k_{\text{states}} = 10$ most relevant states. To summarize the experiences in the retrieval batch we use a forward and backward GRU with 512 hidden units. To train the representation of these, we use auxiliary losses in the form of action, reward, and value prediction (section 2.2). Appendix A.3 provides further details of the setup, training losses, and computational complexity.

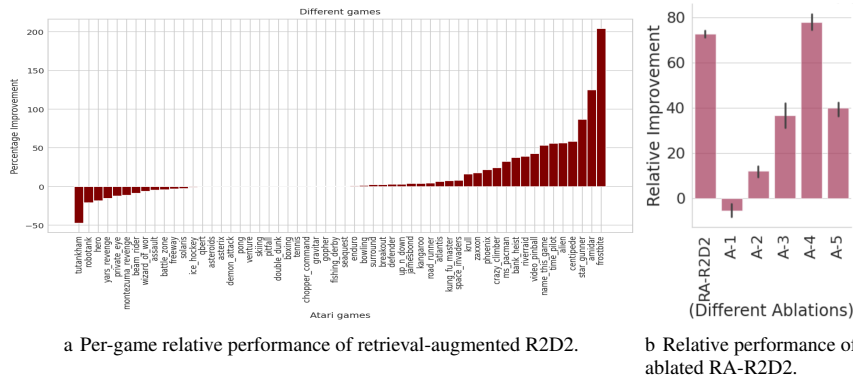


Figure 2: (a) Relative percentage improvement in mean human normalized score of retrieval-augmented R2D2 vs vanilla R2D2 on different Atari games, measured by human normalized score. We report the average score from 3 seeds per method and per game. (b) Relative percentage improvement of ablated RA-R2D2 versus baseline R2D2 for 5 ablations on 10 Atari games. Black lines show standard deviations from 3 seeds.

a Per-game relative performance of retrieval-augmented R2D2.

b Relative performance of ablated RA-R2D2.

3.1. Atari: Single-task off-policy RL

In this experiment, our goal is to evaluate whether retrieval augmentation improves the performance and sample efficiency of a strong, recurrent baseline agent on a challenging, visually-complex environment—the Atari 2600 videogame suite (Bellemare et al., 2013). We use recurrent replay distributed DQN (R2D2, Kapturowski et al. (2018)) as the baseline agent and compare retrieval-augmented R2D2 (RA-R2D2) to vanilla R2D2. The retrieval dataset is the agent’s current replay buffer. The agent process is parameterized as a GRU (Hochreiter & Schmidhuber, 1997), and the retrieval process is parameterized as the slot-based recurrent architecture described in Section 2, using 8 slots. Retrieval batches consist of 256 trajectories from the retrieval dataset.

Overall, we observe an increase of $11.32 \pm 1.2\%$ in the mean human normalized score relative to the R2D2 baseline over 2 billion environment steps, demonstrating that retrieval augmentation is quite beneficial in Atari and that the agent’s own replay buffer is a useful source for retrieval. Raw scores and training curves are presented in Appendix A.4. Figure 2a shows the relative improvement of RA-R2D2 versus the R2D2 baseline. Empirically, retrieval augmentation helps the most in the case of Frostbite, which requires temporally extended planning strategies (Lake et al., 2017). For more discussion, refer to Appendix A.3.5.

3.1.1. ABLATIONS AND ANALYSIS

To understand the benefit of different components of retrieval augmentation, we ablate RA-R2D2 on the 10 Atari games it performs best relative to R2D2. The ablations are as follows, and Figure 2b shows the performance of RA-R2D2 and each ablation relative to the R2D2 baseline.

(A-1) Importance of a separate retrieval process. In R2A, the retrieval process and the agent process are parameterized separately, i.e., they have their own internal states. Here we examine what happens when the agent’s state is used to query the retrieval batch instead of using the retrieval state m_t . To implement this we modify Step 1 of Algorithm 1 to make the query a direct function of the state

of the agent, $q_t = f_{\text{query}}(s_t)$. The resulting query is used in the same way as above. The resulting ablated model is akin to the episodic control baseline of Pritzel et al. (2017).

Conclusion: It is crucial to parameterize the agent process and retrieval process separately, as using the agent state does no better than the baseline. This also shows the benefit of our retrieval formulation as compared to episodic control. Further, Pritzel et al. (2017) observed that direct access to the replay buffer improves performance given low data, but the advantage disappears with more data. Here our experiments show that the agent equipped with retrieval augmentation achieves better results even in the large data regime (2B time-steps).

(A-2) Importance of retrieving information. We examine what happens when the retrieval process does not have access to the retrieval dataset and hence no information is retrieved, keeping all else the same. This ablation thus validates that R2A benefits from retrieval, not from an increase in computation and parameters. Specifically, the retrieval process updates the state of the slots using a transformer (i.e., in Step 1 we replace GRU with a transformer), and the updated state of the transformer is used by the agent process to shape the representation of its value function.

Conclusion: R2A retrieves information that is useful to the agent and its performance gains are not simply due to an increase in model capacity and computation.

(A-3) Shorter retrieved trajectories. We decrease the length of the trajectories that are summarized during retrieval pre-processing, thus reducing the amount of past and future information the retrieval process can retrieve. By default, the trajectories in the retrieval dataset are of length 80. To perform this ablation, we decrease the length of the effective context to only include information from 5 timesteps.

Conclusion: Decreasing the length of the context in the retrieval dataset results in worse performance, thus showing the importance of incorporating contextual information using forward and backward summarization.

(A-4, A-5) Importance of auxiliary losses to summarize retrieval batch. Here we study the use of self-supervised

BERT style masking losses in addition to using action, reward and value prediction. We use these auxiliary losses on top of the representation learned by the forward and the backward dynamics model. To implement these losses, we randomly mask 15% of the hidden states in a trajectory, and then, using the representation of hidden states at other time-steps, we predict the representation of masked hidden states. In A-5, we study using *only* self-supervised BERT style masking losses for summarizing the trajectories.

Conclusion: Ablation A-4 demonstrates that the performance of R2A can further be improved by incorporating BERT style auxiliary losses but that only using BERT style auxiliary losses results in worse performance (but still better than baseline R2D2).

For completeness, Figure 7 in the appendix repeats the ablations on the 5 games that RA-R2D2 performs worst (relative to R2D2). An additional ablation shows that the performance of the R2A can be greatly improved by optimizing hyperparameters for each game separately (A-6), which we did not do for our experiments.

3.2. Gridroboman: Multi-task offline RL with a task-specific retrieval dataset

Beyond querying the agent’s own experiences, retrieval can provide helpful information from other sources of experiences, including experts or other agents, such as in offline RL where the agent must learn from a fixed dataset of experiences generated by other agents without interacting with the environment during training. A major challenge in offline RL is distributional shift—the mismatch between the distribution of states in the training data and those visited by the agent when acting—which makes it difficult to learn an accurate value function for states and actions rarely seen during training. We hypothesize that the retrieval process can improve performance in the offline setting by retrieving trajectories (including states, actions, and rewards) relevant to the agent’s current state, particularly for states and actions that are rare in the offline dataset. We test this hypothesis on a multi-task offline RL setup where a single agent is trained on multiple tasks simultaneously but at evaluation time the retrieval dataset contains only trajectories from the evaluated task.

For this experiment, we created a minimalistic grid-world-based robotic manipulation environment (gridroboman) with 30 tasks related to the three objects (red, green, and blue) on the board. Gridroboman is built on the pycolab game engine (Stepleton et al.). The environment is inspired by the challenges of robotic manipulation, and includes tasks such as “go to object X” and “put object X on object Y”. Details of the environment, its tasks, and an example figure are presented in the appendix (section A.4). Here, we incorporate retrieval augmentation into a vanilla DQN agent as agent-state-recurrence is not needed for this task.

Figure 3 shows the results of training retrieval-augmented DQN (RA-DQN, orange) and DQN (blue) on increasing numbers of tasks. With fewer tasks, RA-DQN and DQN perform identically; however, when the number of training tasks increases the retrieval-augmented agent is able to learn much more effectively than the baseline agent. Training on more tasks requires either additional model capacity or the ability to extract information from fewer relevant samples for each task. By directly querying task-relevant experiences in the offline dataset, retrieval augmentation improves sample efficiency. Note that while the retrieval process does afford extra model capacity to the agent directly, ablation A-2 in section 3.1.1 shows that the retrieved information is what is crucial to performance, not the increased capacity.

3.3. BabyAI: Multi-task offline RL with a multi-task retrieval dataset

Here we evaluate the benefit of retrieval augmentation when data from other tasks is present in the retrieval dataset. Multi-task retrieval data can be either harmful if the retrieved information misguides the agent or beneficial if information from the other tasks is relevant to the current task. Due to the use of attention in the retrieval process, we hypothesize that R2A will be able to retrieve relevant information (and ignore irrelevant information) from other tasks.

To test our hypothesis, we use the BabyAI environment (Chevalier-Boisvert et al., 2018), a partially observable multi-room grid world in which harder tasks are composed of simpler tasks and are formulated using subsets of a synthetic language. At the start of each episode, the agent is placed in a random room and must navigate to a randomly located goal. Due to the partial observability, we use a recurrent DQN (RDQN) agent as the baseline and compare its performance to a retrieval-augmented RDQN (RA-RDQN) agent. More details are provided in Appendix A.5.

As is common in this environment, we measure the success rate of each agent, defined as the ratio of tasks the agent was able to accomplish given a fixed number of steps for each task. Table 1 shows the performance of RA-RDQN with a multi-task replay, RA-RDQN with a replay specific to the current task, and the baseline for varying amounts of offline training data (50K trajectories per task versus 200K trajectories per task). As expected from the previous experiment, retrieval augmentation improves performance over the baseline when using a single-task replay. Performance further improves when using a multi-task replay. We believe that this is due to the compositional nature of tasks in BabyAI, where information about a subtask can be more informative than information about the overall task.

Analysis of retrieved information. To understand this effect better, we analyzed the properties of the retrieved information in the multi-task setting in BabyAI. Out of the

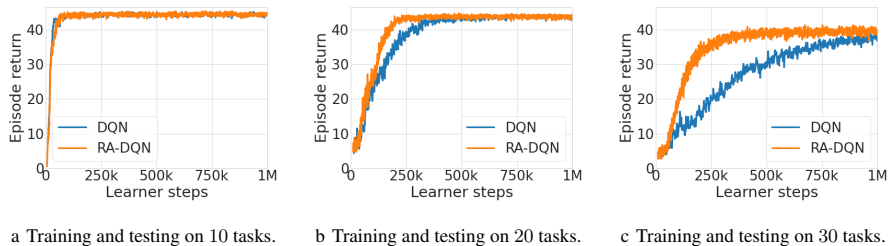


Figure 3: **Gridroboman: Multi-task offline RL with a task-specific retrieval dataset.** Average episode return vs. learner steps for the multi-task gridroboman environment when training and evaluating on 10, 20, and 30 tasks. With fewer tasks (a), the baseline DQN agent (blue) and the retrieval-augmented DQN agent (orange) perform identically; however, when the number of tasks increases (b, c), the retrieval-augmented agent learns much more effectively than the baseline DQN agent. Results are the average of 3 seeds for each method. Curves for individual tasks are shown in the appendix (Figure 9).

Table 1: **BabyAI: Multi-task offline RL with a multi-task retrieval dataset.** Mean success rate of retrieval-augmented recurrent DQN (RA-RDQN) versus a recurrent DQN (RDQN) baseline on the 40 BabyAI levels, as a function of the amount of training data. RA-RDQN is run twice, once with only the current task being evaluated in the retrieval dataset and once with all tasks in it. Results are the average of 3 random seeds with standard errors.

Method	Success Rate (50K)	Success Rate (200K)
RDQN	32% \pm 4%	45% \pm 6%
RA-RDQN (single-task retrieval buffer)	48% \pm 4%	64% \pm 5%
RA-RDQN (multi-task retrieval buffer, without IB)	47% \pm 3%	59% \pm 6%
RA-RDQN (multi-task retrieval buffer)	55% \pm 5%	74% \pm 3%

Table 2: **CausalWorld: Multi-task offline RL with a multi-task retrieval dataset.** Mean success rate of retrieval-augmented behaviour cloning on continuous control task (RA-RDQN) as compared to vanilla behaviour cloning baseline on the 5 tasks. Results are the average of 3 random seeds with standard errors. For more detail, we refer the reader to Appendix A.6.

Method	Success Rate (50K)
BC (behavior cloning)	61% \pm 10%
RA-BC (single-task retrieval buffer)	71% \pm 7%
RA-BC (multi-task retrieval buffer)	82% \pm 5%

40 BabyAI tasks, 15 are compositional—i.e., solving them requires composing information from 2 or more other tasks (e.g., going to the door, fetching a key, etc.). We looked at how often the agent retrieves information from other tasks when solving each task. For the compositional tasks, the agent retrieves information from other tasks 54% of the time, whereas this number is only 21% for the non-compositional tasks. This suggests that the retrieval-augmented agent is retrieving information from other tasks when the current task is compositional and using this information retrieved from relevant sub-tasks to improve its performance.

Information bottleneck ablation. We ran an ablation to validate the use of the information bottleneck (RA-RDQN (multi-task retrieval buffer, without IB)). Table 1 shows the agent performs worse without the information bottleneck (but better than baseline). Such an information bottleneck has been shown to improve generalization (Teh et al., 2017; Goyal et al., 2019a; Galashov et al., 2019).

3.4. CausalWorld: Multi-task offline continuous control

We also evaluate the performance of the R2A on a suite of 5 continuous control object manipulation tasks from the CausalWorld benchmark (Ahmed et al., 2020). We use the same setup for retrieval pre-processing as in BabyAI but use behaviour cloning (BC) as the underlying algorithm, which has been shown to be a strong baseline for offline RL (Gulcehre et al., 2020b). More details are provided in Appendix A.6. We compare the performance of BC to retrieval augmented BC (RA-BC). Table 2 shows the perfor-

mance of the RA-BC with both a multi-task retrieval buffer and a single-task retrieval buffer. Retrieval augmentation improves the performance of BC in both cases.

4. Related Work

Episodic control. The idea of allowing deep RL agents to adapt based on past experiences using a non-parametric memory is not new (Blundell et al., 2016; Pritzel et al., 2017; Hansen et al., 2018; Eysenbach et al., 2019; van Hasselt et al., 2019; Fortunato et al., 2019; Zhu et al., 2020). The basic idea is that the agent is equipped with an episodic memory system, which is used to recall past experiences to inform decisions. There are two important differences between R2A and these methods. (1) In these methods, a local action-value function is constructed by using information about the nearest neighbors in the replay buffer, and then the agent makes a decision about which action to execute based on both the local value function as well as the global value function. However, in the proposed work, we employ a parameterized network (the retrieval process), which has access to the information in the replay buffer, and the agent process uses the retrieved information to shape the predictions of its value function in a fully differentiable way (using attention). (2) In these episodic control methods, there is only one process (the agent), which has direct access to the replay buffer. However, in R2A, the agent has indirect access to the replay buffer via the retrieval process.

Retrieval in language models. Retrieval-based methods have recently been developed for question answering, controllable generation, and machine translation (Guu et al., 2020; Lee et al., 2019; Lewis et al., 2020; Sun et al., 2021;

Borgeaud et al., 2021). The general scheme in such methods is to combine a parametric model (like a BERT-style masked language model or a pre-trained seq2seq model) with a non-parametric retrieval system. These methods share some similarities with our proposed model, since they all involve a retrieval component, but focus on different domains.

Additional related work is discussed in Appendix A.1.

5. Conclusion.

In this work, we developed R2A, an algorithm that augments an RL agent with a retrieval process. The retrieval process and the agent have separate states and shape the representation and predictions of each other via attention. The goal of the retrieval process is to retrieve useful information from a dataset of experiences to help the agent achieve its objective more efficiently and effectively. We show that R2A improves sample efficiency over R2D2, a strong off-policy agent, and compensates for insufficient capacity when training in multi-task offline RL environments. Multiple ablations show the importance of the different components of R2A, including retrieving information from past experiences and parameterizing the agent and retrieval process separately instead of giving the agent process direct access to the replay buffer.

Limitations and Future Work. It would be useful to investigate and extend the proposed idea in these different ways: (a) First, investigate training of the retrieval process and the agent process using different objectives as compared to training them in an end-to-end fashion, (b) Second, scaling R2A to more complex multi-agent problems like in Starcraft (Vinyals et al., 2019), where the retrieval process may be shared between different agents. In R2A, we only query a subset of the retrieval dataset, which limits the generality of the method. (c) Third, even more intriguing would be the possibility of learning an abstract model with abstract internal actions, and rewards, rather than learning a model which queries for information from the retrieval dataset, and hence avoiding the need for Monte Carlo tree search common in the state of the art planning methods (Schrittwieser et al., 2020). (d) Fourth, we don't evaluate the R2A in a few-shot learning setting, where we first pre-train an encoding function of the trajectories in the reply dataset and during test time the agent is exposed to a new task, and needs to use the helper process to adapt faster. We aim to formulate these problems and seek answers in the future work.

6. Acknowledgements

The authors would also like to thank David Silver, Daan Wierstra, Oriol Vinyals, Ivo Danihelka, Hado Van Hasselt, Matthew Botvinick, Thore Graepal, Martin Riedmiller, Pablo Sprechman, Alexander Lerchner, Jane Wang, Rui Zhu, Doina Precup, Andrew Jaegle, Joao Carreira, Fabio

Viola, Raphael Koster, Laurent Sifre, Nando de frietas, Sherjil Ozair, Thomas Hubert, Julian Schrittwieser, Ioannis Antonoglou, Dan Horgan, Peter Battaglia, Jessica Hamrick, Tom Stepleton, Max Jaderberg and Andre Barreto for useful discussions. We would like to thank Bilal Piot, Pablo Sprechmann, Olivier Tieleman for feedback, which helped in improving the clarity of the work. AG would especially like to thank David Silver for many engaging and insightful brainstorming sessions which this work benefited from greatly—the analogy of the retrieval agent as the helper process came about in one such discussion. Lastly, AG would like to thank people at Ferlucci coffee shop in Montreal for their great coffee and interactions, as interactions with them were one of the very few real-life human interactions he had during the course of a remote, virtual internship.

References

- Abdolmaleki, A., Springenberg, J. T., Tassa, Y., Munos, R., Heess, N., and Riedmiller, M. Maximum a posteriori policy optimisation. *arXiv preprint arXiv:1806.06920*, 2018.
- Ahmed, O., Träuble, F., Goyal, A., Neitz, A., Bengio, Y., Schölkopf, B., Wüthrich, M., and Bauer, S. Causalworld: A robotic manipulation benchmark for causal structure and transfer learning. *arXiv preprint arXiv:2010.04296*, 2020.
- Alemi, A. A., Fischer, I., Dillon, J. V., and Murphy, K. Deep variational information bottleneck. *arXiv preprint arXiv:1612.00410*, 2016.
- Allen, J. F. and Koomen, J. A. Planning using a temporal world model. In *Proceedings of the Eighth international joint conference on Artificial intelligence-Volume 2*, pp. 741–747, 1983.
- Arjona-Medina, J. A., Gillhofer, M., Widrich, M., Unterthiner, T., Brandstetter, J., and Hochreiter, S. RUD- DER: Return decomposition for delayed rewards. *arXiv preprint arXiv:1806.07857*, 2018.
- Banino, A., Badia, A. P., Walker, J. C., Scholtes, T., Mitrovic, J., and Blundell, C. Coberl: Contrastive bert for reinforcement learning. In *ICML 2021 Workshop on Un-supervised Reinforcement Learning*, 2021.
- Battaglia, P. W., Pascanu, R., Lai, M., Rezende, D., and Kavukcuoglu, K. Interaction networks for learning about objects, relations and physics. *arXiv preprint arXiv:1612.00222*, 2016.
- Battaglia, P. W., Hamrick, J. B., Bapst, V., Sanchez-Gonzalez, A., Zambaldi, V., Malinowski, M., Tacchetti,

- A., Raposo, D., Santoro, A., Faulkner, R., et al. Relational inductive biases, deep learning, and graph networks. *arXiv preprint arXiv:1806.01261*, 2018.
- Bellemare, M. G., Naddaf, Y., Veness, J., and Bowling, M. The arcade learning environment: An evaluation platform for general agents. *Journal of Artificial Intelligence Research*, 47:253–279, 2013.
- Blundell, C., Uria, B., Pritzel, A., Li, Y., Ruderman, A., Leibo, J. Z., Rae, J., Wierstra, D., and Hassabis, D. Model-free episodic control. *arXiv preprint arXiv:1606.04460*, 2016.
- Borgeaud, S., Mensch, A., Hoffmann, J., Cai, T., Rutherford, E., Millican, K., Driessche, G. v. d., Lespiau, J.-B., Damoc, B., Clark, A., et al. Improving language models by retrieving from trillions of tokens. *arXiv preprint arXiv:2112.04426*, 2021.
- Chen, M., Radford, A., Child, R., Wu, J., Jun, H., Luan, D., and Sutskever, I. Generative pretraining from pixels. In *International Conference on Machine Learning*, pp. 1691–1703. PMLR, 2020a.
- Chen, T., Kornblith, S., Swersky, K., Norouzi, M., and Hinton, G. Big self-supervised models are strong semi-supervised learners. *arXiv preprint arXiv:2006.10029*, 2020b.
- Chevalier-Boisvert, M., Bahdanau, D., Lahlou, S., Willems, L., Saharia, C., Nguyen, T. H., and Bengio, Y. Babyai: A platform to study the sample efficiency of grounded language learning. In *International Conference on Learning Representations*, 2018.
- Cover, T. M. *Elements of information theory*. John Wiley & Sons, 1999.
- Czarnecki, W. M., Pascanu, R., Osindero, S., Jayakumar, S., Swirszcz, G., and Jaderberg, M. Distilling policy distillation. In *The 22nd International Conference on Artificial Intelligence and Statistics*, pp. 1331–1340. PMLR, 2019.
- Dehghani, M., Gouws, S., Vinyals, O., Uszkoreit, J., and Kaiser, Ł. Universal transformers. *arXiv preprint arXiv:1807.03819*, 2018.
- Devlin, J., Chang, M.-W., Lee, K., and Toutanova, K. BERT: Pre-training of deep bidirectional transformers for language understanding. *arXiv preprint arXiv:1810.04805*, 2018.
- Dosovitskiy, A., Beyer, L., Kolesnikov, A., Weissenborn, D., Zhai, X., Unterthiner, T., Dehghani, M., Minderer, M., Heigold, G., Gelly, S., et al. An image is worth 16x16 words: Transformers for image recognition at scale. *arXiv preprint arXiv:2010.11929*, 2020.
- Ernst, D., Geurts, P., and Wehenkel, L. Tree-based batch mode reinforcement learning. *Journal of Machine Learning Research*, 6:503–556, 2005.
- Eysenbach, B., Salakhutdinov, R., and Levine, S. Search on the replay buffer: Bridging planning and reinforcement learning. *arXiv preprint arXiv:1906.05253*, 2019.
- Florensa, C., Duan, Y., and Abbeel, P. Stochastic neural networks for hierarchical reinforcement learning. *arXiv preprint arXiv:1704.03012*, 2017.
- Fortunato, M., Tan, M., Faulkner, R., Hansen, S., Badia, A. P., Buttimore, G., Deck, C., Leibo, J. Z., and Blundell, C. Generalization of reinforcement learners with working and episodic memory. *arXiv preprint arXiv:1910.13406*, 2019.
- Frans, K., Ho, J., Chen, X., Abbeel, P., and Schulman, J. Meta learning shared hierarchies. *arXiv preprint arXiv:1710.09767*, 2017.
- Galashov, A., Jayakumar, S. M., Hasenclever, L., Tirumala, D., Schwarz, J., Desjardins, G., Czarnecki, W. M., Teh, Y. W., Pascanu, R., and Heess, N. Information asymmetry in KL-regularized RL. *arXiv preprint arXiv:1905.01240*, 2019.
- Goyal, A., Brakel, P., Fedus, W., Singhal, S., Lillicrap, T., Levine, S., Larochelle, H., and Bengio, Y. Recall traces: Backtracking models for efficient reinforcement learning. *arXiv preprint arXiv:1804.00379*, 2018.
- Goyal, A., Islam, R., Strouse, D., Ahmed, Z., Botvinick, M., Larochelle, H., Bengio, Y., and Levine, S. Infobot: Transfer and exploration via the information bottleneck. *arXiv preprint arXiv:1901.10902*, 2019a.
- Goyal, A., Lamb, A., Hoffmann, J., Sodhani, S., Levine, S., Bengio, Y., and Schölkopf, B. Recurrent independent mechanisms. *arXiv preprint arXiv:1909.10893*, 2019b.
- Goyal, A., Sodhani, S., Binas, J., Peng, X. B., Levine, S., and Bengio, Y. Reinforcement learning with competitive ensembles of information-constrained primitives. *arXiv preprint arXiv:1906.10667*, 2019c.
- Goyal, A., Bengio, Y., Botvinick, M., and Levine, S. The variational bandwidth bottleneck: Stochastic evaluation on an information budget. *arXiv preprint arXiv:2004.11935*, 2020a.
- Goyal, A., Lamb, A., Gampa, P., Beaudoin, P., Levine, S., Blundell, C., Bengio, Y., and Mozer, M. Object files and schemata: Factorizing declarative and procedural knowledge in dynamical systems. *arXiv preprint arXiv:2006.16225*, 2020b.

- Gulcehre, C., Wang, Z., Novikov, A., Paine, T., Gómez, S., Zolna, K., Agarwal, R., Merel, J. S., Mankowitz, D. J., Paduraru, C., et al. Rl unplugged: A collection of benchmarks for offline reinforcement learning. *Advances in Neural Information Processing Systems*, 33, 2020a.
- Gulcehre, C., Wang, Z., Novikov, A., Paine, T. L., Colmenarejo, S. G., Zolna, K., Agarwal, R., Merel, J., Mankowitz, D., Paduraru, C., et al. Rl unplugged: A suite of benchmarks for offline reinforcement learning. *arXiv preprint arXiv:2006.13888*, 2020b.
- Guu, K., Lee, K., Tung, Z., Pasupat, P., and Chang, M.-W. REALM: Retrieval-augmented language model pre-training. *arXiv preprint arXiv:2002.08909*, 2020.
- Hansen, S., Sprechmann, P., Pritzel, A., Barreto, A., and Blundell, C. Fast deep reinforcement learning using online adjustments from the past. *arXiv preprint arXiv:1810.08163*, 2018.
- Hausman, K., Springenberg, J. T., Wang, Z., Heess, N., and Riedmiller, M. Learning an embedding space for transferable robot skills. In *International Conference on Learning Representations*, 2018.
- Heess, N., Wayne, G., Silver, D., Lillicrap, T., Tassa, Y., and Erez, T. Learning continuous control policies by stochastic value gradients, 2015.
- Heess, N., Wayne, G., Tassa, Y., Lillicrap, T., Riedmiller, M., and Silver, D. Learning and transfer of modulated locomotor controllers. *arXiv preprint arXiv:1610.05182*, 2016.
- Hochreiter, S. and Schmidhuber, J. Long short-term memory. *Neural computation*, 9(8):1735–1780, 1997.
- Jaderberg, M., Mnih, V., Czarnecki, W. M., Schaul, T., Leibo, J. Z., Silver, D., and Kavukcuoglu, K. Reinforcement learning with unsupervised auxiliary tasks. *arXiv preprint arXiv:1611.05397*, 2016.
- Kapturowski, S., Ostrovski, G., Quan, J., Munos, R., and Dabney, W. Recurrent experience replay in distributed reinforcement learning. In *International conference on learning representations*, 2018.
- Ke, N. R., Goyal, A., Bilaniuk, O., Binas, J., Mozer, M. C., Pal, C., and Bengio, Y. Sparse attentive backtracking: Temporal credit assignment through reminding. In *Advances in Neural Information Processing Systems*, pp. 7640–7651, 2018.
- Ke, N. R., Singh, A., Touati, A., Goyal, A., Bengio, Y., Parikh, D., and Batra, D. Learning dynamics model in reinforcement learning by incorporating the long term future. *arXiv preprint arXiv:1903.01599*, 2019.
- Kingma, D. P. and Welling, M. Auto-encoding variational Bayes. *arXiv preprint arXiv:1312.6114*, 2013.
- Kolodner, J. L. An introduction to case-based reasoning. *Artificial intelligence review*, 6(1):3–34, 1992.
- Lake, B. M., Ullman, T. D., Tenenbaum, J. B., and Gershman, S. J. Building machines that learn and think like people. *Behavioral and brain sciences*, 40, 2017.
- Leake, D. B. Case-based reasoning: experiences, lessons, and future directions. 1996.
- Lee, K., Chang, M.-W., and Toutanova, K. Latent retrieval for weakly supervised open domain question answering. *arXiv preprint arXiv:1906.00300*, 2019.
- Lewis, P., Perez, E., Piktus, A., Petroni, F., Karpukhin, V., Goyal, N., Küttler, H., Lewis, M., Yih, W.-t., Rocktäschel, T., et al. Retrieval-augmented generation for knowledge-intensive nlp tasks. *arXiv preprint arXiv:2005.11401*, 2020.
- Lillicrap, T. P., Hunt, J. J., Pritzel, A., Heess, N., Erez, T., Tassa, Y., Silver, D., and Wierstra, D. Continuous control with deep reinforcement learning. *arXiv preprint arXiv:1509.02971*, 2015.
- Lin, L.-J. Self-improving reactive agents based on reinforcement learning, planning and teaching. *Machine learning*, 8(3-4):293–321, 1992.
- Liu, S., Lever, G., Wang, Z., Merel, J., Eslami, S., Hennes, D., Czarnecki, W. M., Tassa, Y., Omidshafiei, S., Abdolmaleki, A., et al. From motor control to team play in simulated humanoid football. *arXiv preprint arXiv:2105.12196*, 2021.
- Liu, Z., Li, X., Kang, B., and Darrell, T. Regularization matters in policy optimization. 2019.
- Logan, G. D., Cox, G. E., Annis, J., and Lindsey, D. R. The episodic flanker effect: Memory retrieval as attention turned inward. *Psychological Review*, 128(3):397, 2021.
- Mazouze, B., Combes, R. T. d., Doan, T., Bachman, P., and Hjelm, R. D. Deep reinforcement and infomax learning. *arXiv preprint arXiv:2006.07217*, 2020.
- Merel, J., Botvinick, M., and Wayne, G. Hierarchical motor control in mammals and machines. *Nature communications*, 10(1):1–12, 2019.
- Mnih, V., Kavukcuoglu, K., Silver, D., Rusu, A. A., Veness, J., Bellemare, M. G., Graves, A., Riedmiller, M., Fidjeland, A. K., Ostrovski, G., Petersen, S., Beattie, C., Sadik, A., Antonoglou, I., King, H., Kumaran, D., Wierstra, D., Legg, S., and Hassabis, D. Human-level control through deep reinforcement learning. *Nature*, 518(7540):529–533, February 2015a.

- Mnih, V., Kavukcuoglu, K., Silver, D., Rusu, A. A., Veness, J., Bellemare, M. G., Graves, A., Riedmiller, M., Fidjeland, A. K., Ostrovski, G., et al. Human-level control through deep reinforcement learning. *nature*, 518(7540): 529–533, 2015b.
- Nair, A., Dalal, M., Gupta, A., and Levine, S. AWAC: Accelerating online reinforcement learning with offline datasets. 2020.
- Pascanu, R., Li, Y., Vinyals, O., Heess, N., Buesing, L., Racanière, S., Reichert, D., Weber, T., Wierstra, D., and Battaglia, P. Learning model-based planning from scratch. *arXiv preprint arXiv:1707.06170*, 2017.
- Pertsch, K., Lee, Y., and Lim, J. J. Accelerating reinforcement learning with learned skill priors. *arXiv preprint arXiv:2010.11944*, 2020.
- Pritzel, A., Uria, B., Srinivasan, S., Badia, A. P., Vinyals, O., Hassabis, D., Wierstra, D., and Blundell, C. Neural episodic control. In *International Conference on Machine Learning*, pp. 2827–2836. PMLR, 2017.
- Racanière, S., Weber, T., Reichert, D. P., Buesing, L., Guez, A., Rezende, D., Badia, A. P., Vinyals, O., Heess, N., Li, Y., et al. Imagination-augmented agents for deep reinforcement learning. In *Proceedings of the 31st International Conference on Neural Information Processing Systems*, pp. 5694–5705, 2017.
- Radford, A., Wu, J., Child, R., Luan, D., Amodei, D., Sutskever, I., et al. Language models are unsupervised multitask learners. *OpenAI blog*, 1(8):9, 2019.
- Rezende, D. J., Mohamed, S., and Wierstra, D. Stochastic backpropagation and approximate inference in deep generative models. In *International conference on machine learning*, pp. 1278–1286. PMLR, 2014.
- Riedmiller, M. Neural fitted Q iteration—first experiences with a data efficient neural reinforcement learning method. In *European conference on machine learning*, pp. 317–328. Springer, 2005.
- Schrittwieser, J., Antonoglou, I., Hubert, T., Simonyan, K., Sifre, L., Schmitt, S., Guez, A., Lockhart, E., Hassabis, D., Graepel, T., et al. Mastering atari, go, chess and shogi by planning with a learned model. *arXiv preprint arXiv:1911.08265*, 2019.
- Schrittwieser, J., Antonoglou, I., Hubert, T., Simonyan, K., Sifre, L., Schmitt, S., Guez, A., Lockhart, E., Hassabis, D., Graepel, T., et al. Mastering atari, go, chess and shogi by planning with a learned model. *Nature*, 588(7839): 604–609, 2020.
- Siegel, N. Y., Springenberg, J. T., Berkenkamp, F., Abdolmaleki, A., Neunert, M., Lampe, T., Hafner, R., Heess, N., and Riedmiller, M. Keep doing what worked: Behavioral modelling priors for offline reinforcement learning. *arXiv preprint arXiv:2002.08396*, 2020.
- Silver, D. Reinforcement learning and simulation-based search in computer go. 2009.
- Silver, D., Sutton, R. S., and Müller, M. Sample-based learning and search with permanent and transient memories. In *Proceedings of the 25th international conference on Machine learning*, pp. 968–975, 2008.
- Silver, D., Huang, A., Maddison, C. J., Guez, A., Sifre, L., Van Den Driessche, G., Schrittwieser, J., Antonoglou, I., Panneershelvam, V., Lanctot, M., et al. Mastering the game of go with deep neural networks and tree search. *nature*, 529(7587):484–489, 2016.
- Silver, D., Hasselt, H., Hessel, M., Schaul, T., Guez, A., Harley, T., Dulac-Arnold, G., Reichert, D., Rabinowitz, N., Barreto, A., et al. The predictron: End-to-end learning and planning. In *International Conference on Machine Learning*, pp. 3191–3199. PMLR, 2017.
- Silver, D., Hubert, T., Schrittwieser, J., Antonoglou, I., Lai, M., Guez, A., Lanctot, M., Sifre, L., Kumaran, D., Graepel, T., et al. A general reinforcement learning algorithm that masters chess, shogi, and go through self-play. *Science*, 362(6419):1140–1144, 2018.
- Springenberg, J. T., Heess, N., Mankowitz, D., Merel, J., Byravan, A., Abdolmaleki, A., Kay, J., Degraeve, J., Schrittwieser, J., Tassa, Y., et al. Local search for policy iteration in continuous control. *arXiv preprint arXiv:2010.05545*, 2020.
- Stepleton, T., Delalleau, O., Ostrovski, G., and Wenke, S. URL <https://github.com/deepmind/pycolab>.
- Strouse, D., Kleiman-Weiner, M., Tenenbaum, J., Botvinick, M., and Schwab, D. Learning to share and hide intentions using information regularization. *arXiv preprint arXiv:1808.02093*, 2018.
- Sun, Y., Wang, S., Feng, S., Ding, S., Pang, C., Shang, J., Liu, J., Chen, X., Zhao, Y., Lu, Y., et al. Ernie 3.0: Large-scale knowledge enhanced pre-training for language understanding and generation. *arXiv preprint arXiv:2107.02137*, 2021.
- Sutton, R. S. Dyna, an integrated architecture for learning, planning, and reacting. *ACM Sigart Bulletin*, 2(4):160–163, 1991.

- Teh, Y., Bapst, V., Czarnecki, W. M., Quan, J., Kirkpatrick, J., Hadsell, R., Heess, N., and Pascanu, R. Distral: Robust multitask reinforcement learning. In *Advances in Neural Information Processing Systems*, pp. 4496–4506, 2017.
- Tishby, N., Pereira, F. C., and Bialek, W. The information bottleneck method. *arXiv preprint physics/0004057*, 2000.
- Van Hasselt, H., Guez, A., and Silver, D. Deep reinforcement learning with double q-learning. In *Proceedings of the AAAI conference on artificial intelligence*, volume 30, 2016.
- van Hasselt, H. P., Hessel, M., and Aslanides, J. When to use parametric models in reinforcement learning? *Advances in Neural Information Processing Systems*, 32:14322–14333, 2019.
- Vaswani, A., Shazeer, N., Parmar, N., Uszkoreit, J., Jones, L., Gomez, A. N., Kaiser, Ł., and Polosukhin, I. Attention is all you need. In *Advances in neural information processing systems*, pp. 5998–6008, 2017.
- Vecerik, M., Hester, T., Scholz, J., Wang, F., Pietquin, O., Piot, B., Heess, N., Rothörl, T., Lampe, T., and Riedmiller, M. Leveraging demonstrations for deep reinforcement learning on robotics problems with sparse rewards. *arXiv preprint arXiv:1707.08817*, 2017.
- Veerapaneni, R., Co-Reyes, J. D., Chang, M., Janner, M., Finn, C., Wu, J., Tenenbaum, J., and Levine, S. Entity abstraction in visual model-based reinforcement learning. In *Conference on Robot Learning*, pp. 1439–1456. PMLR, 2020.
- Vezhnevets, A. S., Osindero, S., Schaul, T., Heess, N., Jaderberg, M., Silver, D., and Kavukcuoglu, K. Feudal networks for hierarchical reinforcement learning. In *International Conference on Machine Learning*, pp. 3540–3549. PMLR, 2017.
- Vinyals, O., Babuschkin, I., Czarnecki, W. M., Mathieu, M., Dudzik, A., Chung, J., Choi, D. H., Powell, R., Ewalds, T., Georgiev, P., et al. Grandmaster level in starcraft II using multi-agent reinforcement learning. *Nature*, 575 (7782):350–354, 2019.
- Watters, N., Matthey, L., Bosnjak, M., Burgess, C. P., and Lerchner, A. Cobra: Data-efficient model-based rl through unsupervised object discovery and curiosity-driven exploration. *arXiv preprint arXiv:1905.09275*, 2019.
- Wayne, G., Hung, C.-C., Amos, D., Mirza, M., Ahuja, A., Grabska-Barwinska, A., Rae, J., Mirowski, P., Leibo, J. Z., Santoro, A., et al. Unsupervised predictive memory in a goal-directed agent. *arXiv preprint arXiv:1803.10760*, 2018.
- Weisz, G., Amortila, P., and Szepesvári, C. Exponential lower bounds for planning in mdps with linearly-realizable optimal action-value functions. In *Algorithmic Learning Theory*, pp. 1237–1264. PMLR, 2021.
- Zambaldi, V., Raposo, D., Santoro, A., Bapst, V., Li, Y., Babuschkin, I., Tuyls, K., Reichert, D., Lillicrap, T., Lockhart, E., et al. Deep reinforcement learning with relational inductive biases. In *International Conference on Learning Representations*, 2018.
- Zhu, G., Lin, Z., Yang, G., and Zhang, C. Episodic reinforcement learning with associative memory. 2020.

A. Appendix

Contents

A.1. Extended Relevant Work.

Model-based RL. There are different ways to integrate knowledge across past experiences. One of the most common way is by learning a model of the world, and using the predictions from the model to improve the policy and the value function (Sutton, 1991; Silver et al., 2008; Silver, 2009; Allen & Koomen, 1983; Silver et al., 2016; Pascanu et al., 2017; Racanière et al., 2017; Silver et al., 2018; Springenberg et al., 2020; Schrittwieser et al., 2020). To integrate information across different episodes (potentially separated by many time-steps), a model may need to be unrolled for many time-steps leading to compounding errors. In R2A, the agent has direct access to the information in the retrieval dataset, and querying across multiple trajectories (in parallel) in the retrieval dataset potentially separated by hundreds of time-steps.

Structural Inductive Biases. Deep learning has proposed structural inductive biases such as Transformers (Vaswani et al., 2017; Dehghani et al., 2018; Radford et al., 2019; Chen et al., 2020a;b; Dosovitskiy et al., 2020) or slot based recurrent architectures (Battaglia et al., 2016; Zambaldi et al., 2018; Battaglia et al., 2018; Goyal et al., 2019b; Watters et al., 2019; Goyal et al., 2020b; Veerapaneni et al., 2020) where the induced structure has improved generalization, model-size scaling, and long-range dependencies.

Reinforcement Learning with Offline Datasets. Recent work in RL has tried exploiting large datasets collected across many tasks to improve the sample efficiency of RL algorithms (Vecerik et al., 2017; Pertsch et al., 2020; Nair et al., 2020; Siegel et al., 2020). An advantage of such large datasets is that they can be collected cheaply, and can then be reused for learning many downstream tasks. A general scheme for exploiting information about such task-agnostic datasets is either using them to directly improve the value function, or by extracting a set of skills or options and learning new tasks by recombining them. In our work, we try to use information in the replay buffer by querying and searching for the relevant information across multiple trajectories which otherwise would take many replays through coincidentally relevant information for this to occur.

Separation of concerns. In Hierarchical RL (HRL) (Heess et al., 2016; Frans et al., 2017; Vezhnevets et al., 2017; Florensa et al., 2017; Hausman et al., 2018; Goyal et al., 2019c), there’s separation of concerns among different policies, each policy focuses on a different aspect of the task, e.g., giving task relevant information to the high level policy only such that low level policy learns behaviours that are task agnostic. In these methods, the high level policy shapes the behaviour of low level policy by either influencing representations or by influencing rewards.

It is possible to view our work through an analogous lens: wherein the “retrieval process” is the higher level policy (and has access to all the information in the replay buffer) and is influencing the representation of the agent process that is interacting with the environment. However, there are also notable differences in our work—for instance, the agent process also directly shapes the representation of the retrieval process, which is generally not the case in HRL (e.g., in Vezhnevets et al. (2017) the manager directly influences the worker, but the worker does not directly influence the manager).

Efficient Credit assignment. Learning long term dependencies requires assigning credit to time-steps far back in the past. Common methods for assigning credit in dynamics model like backpropagation through time requires information to be propagated backwards through every single step in the past. This could become computationally expensive when used with very long sequences. Methods which try to get around this problem only back-propagate information through a selected time-steps in the past, realized by a learned mechanism that associates current state with relevant past states (Ke et al., 2018; Wayne et al., 2018; Arjona-Medina et al., 2018; Goyal et al., 2018; Fortunato et al., 2019). Most of these works consider assigning credit to states within the same trajectory, whereas the proposed model R2A, searches for the relevant information in the replay buffer which includes information from other trajectories also.

Memory retrieval as attention turned inward. The proposed work also validates the conjecture put forward in (Logan et al., 2021): *Perceiving and remembering pose the same computational problems: desired information must be extracted from complex multidimensional structures. The conjecture is that the extraction process is selective attention. Turned outward, it retrieves information from perception. Turned inward, it retrieves information from memory.*

A.2. Information Theoretic Formulation

Let’s denote the agent’s policy $\pi_\theta(A | S, G)$, where S is the agent’s state, A the agent’s action, G the information from the retrieval process conditioned on the current state of the agent i.e., $G = f_{\text{retrieval}}(S)$, and θ the parameters of the neural network representing the policy. We want to train agents that in addition to maximizing reward, minimize the policy dependence on the information from the retrieval process, quantified by the conditional mutual information $I(A; G | S)$.

This approach of minimizing the dependence of the policy on the information from the retrieval process can be interpreted as encouraging agents to learn useful behaviours and to follow those behaviours closely, except where diverting from doing so (as a result of using information from the retrieval process) leads to higher reward (Strouse et al., 2018; Teh et al., 2017; Goyal et al., 2019a; Galashov et al., 2019; Czarnecki et al., 2019). To see this, note that the conditional mutual information can also be written as $I(A; G | S) = \mathbb{E}_{\pi_\theta} [D_{\text{KL}}[\pi_\theta(A | S, G) | \pi_0(A | S)]]$ where \mathbb{E}_{π_θ} denotes an expectation over trajectories, $\pi_0(A | S) = \sum_g p(g) \pi_\theta(A | S, g)$. is a “default” policy with the information from the retrieval process marginalized out. We maximize the following objective:

$$\begin{aligned} J(\theta) &\equiv \mathbb{E}_{\pi_\theta} [r] - \beta I(A; G | S) \\ &= \mathbb{E}_{\pi_\theta} [r - \beta D_{\text{KL}}[\pi_\theta(A | S, G) | \pi_0(A | S)]], \end{aligned} \quad (1)$$

where $\beta > 0$ is a tradeoff parameter, \mathbb{E}_{π_θ} denotes an expectation over trajectories (for ex. generated by the agent’s policy) and D_{KL} refers to the Kuhlback-Leibler divergence.

(Goyal et al., 2019a; Galashov et al., 2019) proposes to optimize the Eq. 1 by maximizing the lower bound $\tilde{J}(\theta)$ ³:

$$J(\theta) \geq \tilde{J}(\theta) \equiv \mathbb{E}_{\pi_\theta} [r - \beta D_{\text{KL}}[p_{\text{enc}}(Z | S, G) | q(Z | S)]] . \quad (2)$$

We parameterize the policy $\pi_\theta(A | S, G)$ using an encoder $p_{\text{enc}}(Z | S, G)$, a decoder $p_{\text{dec}}(A | S, Z)$ and the $q(Z | S)$ is the learned prior such that $\pi_\theta(A | S, G) = \sum_z p_{\text{enc}}(z | S, G) p_{\text{dec}}(A | S, z)$.⁴ The encoder output Z is meant to represent the information from the retrieval process that the agent believes is important to access in the present state S in order to perform well.

Due to the data processing inequality (DPI) (Cover, 1999) $I(Z; G | S) \geq I(A; G | S)$, and hence to obtain an upper bound on $I(Z; G | S)$, we must first obtain an upper bound on $I(Z; G | S = s)$, and then average over $p(s)$. We get the following result:

$$I(Z; G | S) \leq \sum_s p(s) \sum_g p(g | s) D_{\text{KL}}(p(Z | s, g) || r(Z)) \quad (3)$$

Such an information bottleneck has shown to improve generalization (Teh et al., 2017; Goyal et al., 2019a;c; Galashov et al., 2019; Merel et al., 2019; Liu et al., 2019; Goyal et al., 2020a; Liu et al., 2021).

A.3. Atari: Implementation details and raw scores for R2D2 and RA-R2D2.

Table 4 shows the raw scores achieved by RA-R2D2 and the R2D2 baseline. For R2D2 baseline and for the parameterization of the agent process, we follow the exact same training setup as in (Banino et al., 2021). Figure ??, ??, ??, shows the learning curve for both the proposed model and the R2D2 baseline for different games.

Training Losses:

- The parameters of the state encoder are trained by the RL loss and the auxiliary losses used to train the forward/backward summarizer. The state encoder encodes information about the past actions, past rewards and the current observation into an abstract state.
- The parameters of the retrieval process are trained by the RL loss and the information bottleneck regularizer.
- The parameters of the agent process are trained only by the RL loss.

³We ask the reader to refer to Information Theoretic Formulation section in the appendix.

⁴For experiments, we estimate the the marginals and conditionals using a single sample throughout.

Hyperparameters:

- At each learner step, the agent samples a large batch of 512 trajectories from the replay buffer. A fixed fraction of the batch (64 trajectories) is used for learning the Q-function and the remaining trajectories forms the retrieval batch.
- We sample a different retrieval dataset for each gradient update. The re-encoding of the trajectories is performed for each gradient update during training.
- The retrieval process selects the top- $k_{\text{traj}} = 10$ most relevant trajectories (in step 2, section 2.3), and then retrieves relevant information from the selected trajectories (step 3, section 2.3) using the top- $k_{\text{states}} = 10$ most relevant states (see 4).
- To summarize the experiences in the retrieval batch we use a forward and backward GRU with 512 hidden units.
- We use 8 slots for Atari-R2D2 experiments.
- We use auxiliary losses in the form of action or policy prediction (section 2.2). We follow the same setup as proposed in (Schrittwieser et al., 2020).
- The value of the β coefficient for the information bottleneck regularizer is fixed to 0.1.
- The rest of the hyperparameters for R2D2 are taken from (Kapturowski et al., 2018) and are detailed in table 3

Hyperparameter	Value
Optimizer	Adam
Learning rate	0.0001
Q's λ	0.8
Adam epsilon	10^{-7}
Adam beta1	0.9
Adam beta2	0.999
Adam clip norm	40
Q-value transform	$h(x) = \text{sign}(x)(\sqrt{ x + 1} - 1) + \epsilon x$
Discount factor	0.997
Trace length (Atari)	80
Replay period (Atari)	40
Replay capacity	100000 sequences
Replay priority exponent	0.9
Importance sampling exponent	0.6
Minimum sequences to start replay	5000
Target Q-network update period	400
Evaluation ϵ	0.01
Target ϵ	0.01

Table 3: Hyperparameters used in the Atari R2D2 experiments.

Implementation details:

- We use GRU style gating and layernorm whenever we are changing the state of the agent process or the state of the slots in a residual way (Step 5, 6 in Algorithm 1).
- If the input to a neural network f_{nn} consists of two tensors x, y , we never concatenate the inputs to the neural network. We make use of attention. We assume one of the inputs is the primary input (lets say x), and other input is privileged input (as a result of doing some expensive computation, let's say y). First, we compute $f_{nn}(x)$, and then using the output of this computation, we cross-attend over y using multi-head attention.
- When computing the forward summary of the trajectories in the retrieval batch $h = h_t + s_t$, we also add the information about the current encoded state i.e., s_t . Here we also use GRU style gating.

Visual Encoder Visual observations are encoded using a ResNet-47 encoder. The 47 layers are divided in 4 groups which have the following characteristics:

- An initial stride-2 convolution with filter size 3×3 ($1 \cdot 4$ layers).
- Number of residual bottleneck blocks (in order): $(2, 4, 6, 2)$. Each block has 3 convolutional layers with ReLU activations, with filter sizes 1×1 , 3×3 , and 1×1 respectively $((2 + 4 + 6 + 2) \cdot 3$ layers).
- Number of channels for the last convolution in each block: $(64, 128, 256, 512)$.
- Number of channels for the non-last convolutions in each block: $(16, 32, 64, 128)$.
- Group norm is applied after each group, with a group size of 8.

After this observation encoding step, a final layer with ReLU activations of sizes 512 is applied.

Computational Complexity. Here we discuss the computational complexity of the R2A.

The following computations are happening at each step within a trajectory:

- A particular slot selects the relevant trajectories and relevant states at each time-step.
- We use an attention mechanism to select the set of relevant trajectories and relevant states. This process scales with the number of trajectories in the retrieval batch.
- The set of relevant trajectories and relevant states changes across different time-steps within a trajectories. This process is repeated for all the slots independently, but can be efficiently performed on GPUs/TPUs.

We made following optimizations to reduce the computational complexity of the R2A.

- For Atari and Gridroboman experiments instead of using a learned attention mechanism to rank the trajectories (in step 2, section 2.3), we can also just use those trajectories which are of high return (Abdolmaleki et al., 2018) since we already know that the data in the retrieval dataset is specific to the task on which we are training the agent.
- Once we have selected relevant trajectories, we can further reduce the computational cost of selecting most relevant states (in the selected trajectories) by only considering those states which are semantically similar to the agent's current state.

Improvements tried that seem to improve the performance but were not evaluated exhaustively:

- Instead of performing only single step of retrieval at each step, we can also query the replay buffer multiple times within a time-step at the cost of increased computational complexity.
- We can allow different slots to retrieve information at different time scales.

We note that all of the hyperparameters for the retrieval process, except for the number of trajectories in the retrieval batch, remain the same across all experiments (Atari, gridroboman, and BabyAI).

A.3.1. RETRIEVAL PROCESS: RETRIEVING INFORMATION FROM THE RETRIEVAL BUFFER.

Here we discuss the different steps involved in retrieving information from the retrieval buffer:

Query computation. Each slot independently computes its prestate using the contextual information from the agent using a GRU. Then, each slot independently computes a *retrieval query* which will be matched against information in the retrieval buffer.

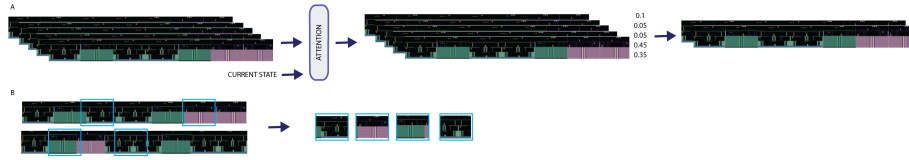


Figure 4: Retrieval of most relevant trajectories and states. A) The retrieval process selects the top- $k_{tra,j}$ most relevant trajectories as specified in step 2, section 2.3. In the figure scalars represent attention weights. B) Then the retrieval process retrieves relevant information from the selected trajectories by selecting the most relevant states from the top- k trajectories as detailed in step 3, section 2.3

Identification of most relevant trajectories and states for each slot. The retrieval mechanism process uses an attention mechanism to match a query produced by the the retrieval state associated with each slot to keys computed on each time step of each trajectory of the retrieval batch. This process assigns a single scalar to each state within a trajectory. These scores are used to assign a scalar to each trajectory and then normalized across trajectories. These normalized scores are then used by the retrieval process to select the top- $k_{tra,j}$ most relevant trajectories (see Figure. 4). The process is then again repeated to select most relevant states with the selected trajectories. Here, a single scalar is assigned to each state with in selected trajectories and then normalized across all the states. These scores are then used to select most relevant states within the most relevant trajectories.

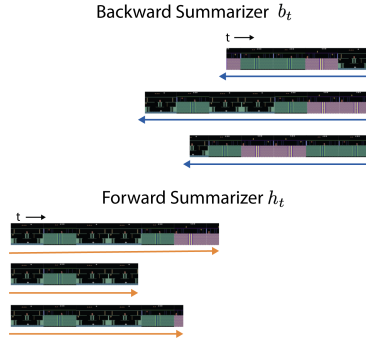


Figure 5: Each trajectory in the retrieval batch is summarized via a forward and a backward running parametric structured model (Transformers or slot based recurrent network). Each state in the trajectory is represented by a (h_t, b_t) tuple where h_t represents the summary of the past and b_t represents the summary of the future with that trajectory.

Information retrieval from the most relevant states. In the previous step, we selected most relevant states within the most relevant trajectories. Now we integrate information across the selected states. We again use the attention mechanism. Here the query by the slots is matched against the keys (which are the function of the forward running dynamics model), to retrieve information about the future (and values are the function of the backward running dynamics model). See figure. 5 for more details.

Retrieval Augmented Reinforcement Learning

Environment	R2D2	RA-R2D2
Alien	52268 ± 4125	81626 ± 5123
Amidar	10976 ± 2341	24693 ± 1982
Assault	45521 ± 4751	43497 ± 6653
Asterix	997910 ± 51241	997585 ± 89251
Asteroids	262560 ± 94168	254194 ± 72141
Atlantis	1424723 ± 67589	1516463 ± 98140
BankHeist	3923 ± 512	19397 ± 5931
BattleZone	590913 ± 128715	466783 ± 89724
BeamRider	89038 ±	79241 ±
Bowling	250.37 ±	253.5 ±
Boxing	99 ± 0	99 ± 0
Breakout	848 ± 121	869 ± 51
Centipede	315329 ± 151612	497746 ± 12515
ChopperCommand	998842 ± 11451	999936 ± 3422
CrazyClimber	184132 ± 12912	226469 ± 9251
Defender	538752 ± 18241	554158 ± 21415
DemonAttack	143552 ± 0	143519 ± 0
DoubleDunk	24 ± 0	24 ± 0
Enduro	2332 ± 32	2359 ± 19
FishingDerby	71.357 ± 2.51	73.13 ± 3.12
Freeway	34 ± 0	33.19 ± 0
Frostbite	168225 ± 51891	511159 ± 124512
Gopher	123138 ± 4121	123841 ± 8914
Gravitar	13142 ± 1214	13198 ± 1102
Hero	43257 ± 4121	35431 ± 2412
IceHockey	72.74 ± 31	71.59 ± 12
Jamesbond	24873 ± 2141	25873 ± 2817
Kangaroo	14614	15232
Krull	158509 ± 21415	183921 ± 31415
KungFuMaster	208583 ± 2102	224385 ± 41512
MontezumaRevenge	1966.7 ± 987	1750 ± 1800
MsPacman	33530 ± 1214	44396 ± 4521
NameThisGame	30232 ± 3151	45140 ± 2412
Phoenix	695251 ± 32515	847914 ± 12415
Pitfall	0.0 ± 0	0.0 ± 0
Pong	21 ± 0	21 ± 0
PrivateEye	21602 ± 4124	18923 ± 2415
Qbert	242169 ± 51512	241525 ± 32513
Riverraid	32441 ± 5314	44554 ± 7325
RoadRunner	490872 ± 51512	513521 ± 65132
Robotank	128.44 ± 18	102 ± 29
Seaquest	998664 ± 1212	999899 ± 51
Skiing	-29973 ±	1212 -29232 ± 2412
Solaris	3924 ± 3415	3853 ± 1241
SpaceInvaders	57198 ± 14125	62624 ± 4215
StarGunner	256129 ±	478231 ±
Surround	9.52 ± 0	10 ± 0
Tennis	7.16 ± 0	0 ± 0
TimePilot	168592 ± 21241	260609 ± 41212
Tutankham	390 ± 41	235 ± 89
UpNDown	544439 ± 5851	561389 ± 21516
Venture	2000 ± 0	2000 ± 0
VideoPinball	673679 ±	234151 962119 ± 24151
WizardOfWor	78431 ± 5159	73500 ± 6231
Yars Revenge	674692 ± 125116	513549 ± 89151
Zaxxon	53312 ± 15152	62631 ± 5161

Table 4: Scores obtained on different atari games. (average over 3 different seeds).

Retrieval Augmented Reinforcement Learning

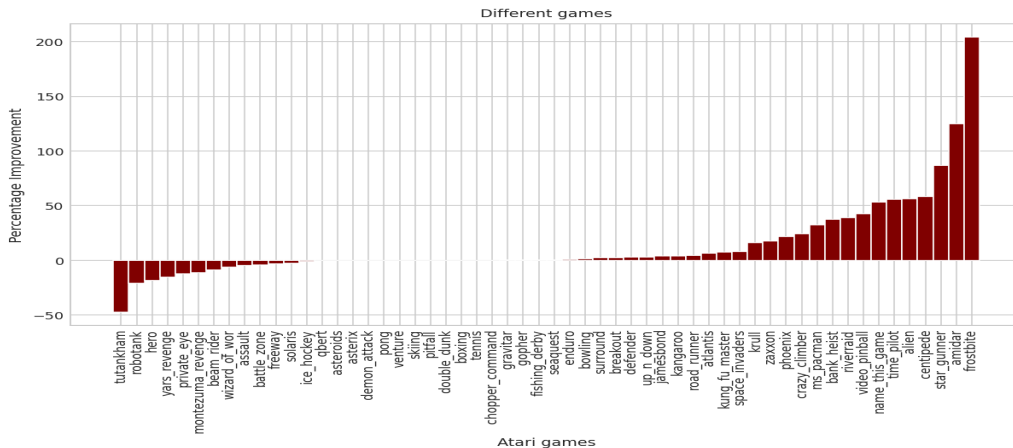


Figure 6: Relative improvement of retrieval-augmented R2D2 vs vanilla R2D2 on different Atari games, measured by human normalized score. We report the average score from 3 seeds per method and per game.

A.3.2. DETAILS ON ABLATIONS

Ablation A-1: In this ablation, the internal retrieval state, \mathbf{m}_t is removed. The query \mathbf{q}_t is computed from \mathbf{s}_t directly as $\mathbf{q}_t = f_{\text{query}}(\mathbf{s}_t)$. The retrieval vector \mathbf{g}_t is computed as per steps 2-4 of the original algorithm. Step 5 does not occur, and in step 6 the only update is $\mathbf{s}_t \leftarrow \mathbf{s}_t + \mathbf{g}_t$.

Ablation A-2: In this ablation, there is no retrieval batch. The retrieval process is parametrized as before with a n_k -slot memory. Step 1 is identical, but steps 2-4 do not occur. Memory slots are updated as per the joint update of step 5. Step 6 is otherwise identical, except that keys and values are computed from the memory slots \mathbf{m}_t^k instead of the retrieved values \mathbf{z}_t^k .

Ablation A-3: In this ablation, the length of the trajectories used for summarization is reduced from 80 to 5. The trajectories used for Q learning are unchanged.

Ablations A-4 and A-5: In our experiments, we use standard policy, reward and value prediction cross-entropy losses (Schrittwieser et al., 2020) to train the forward and backward summarizers. In A-4, we add a BERT loss; tokens are obtained by compressing the agent states \mathbf{s}_t with VQ-VAE. In A-5, we only use the BERT loss.

A.3.3. ADDITIONAL ATARI ABLATIONS

Here we perform ablations on RA-R2D2 using the 5 Atari games on which RA-R2D2 performs worst relative to baseline R2D2. Figure 7 shows the relative performance of different ablations compared to the R2D2 baseline. Ablations 1-5 are as described in the main text (section 3.1.1). For these results, we also ran a sixth ablation.

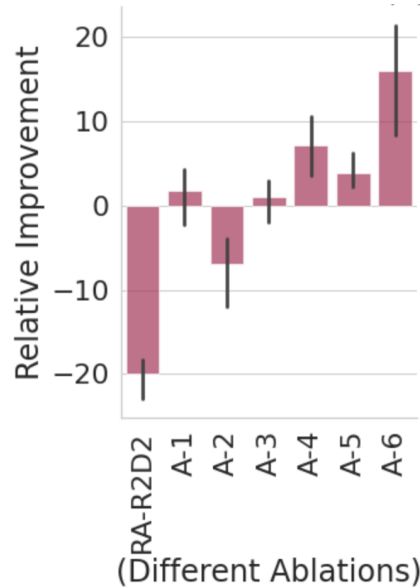


Figure 7: Relative performance of ablated RA-R2D2 versus baseline R2D2 for 6 ablations on 5 Atari games on which RA-R2D2 performs worse than baseline R2D2.

Role of k_{traj} and k_{states} (A-6). In our experiments, the retrieval process selects the top $k_{\text{traj}} = 10$ most relevant trajectories (step 2, section 2.3) and then selects the top $k_{\text{states}} = 10$ most relevant states of these trajectories (step 3, section 2.3) from which to retrieve relevant information. To better understand the role of these hyperparameters, we independently vary these two hyper-parameters (top k_{traj} and top k_{states}) over the values $\{5, 10, 20\}$. Figure 7 shows that after independently varying these two hyper-parameters the performance of the R2A can be improved as compared to the R2D2 baseline.

A.3.4. EPISODIC CONTROL BASELINE

Comparison to Episodic Control baselines. We have performed ablations where we compared to the scenario where we just keep the simple episodic memory (refer to section. 3.1.1, ablation A-1). The result of ablations shows that for R2D2 accessing the dataset in a non-parametric way actually hurts the performance of the RL algorithm

A.3.5. RETRIEVAL AUGMENTED RL HELPING FROSTBITE

Empirically, we found that the proposed method helps the most in the case of Frostbite. In Frostbite, players control an agent (Frostbite Bailey) tasked with constructing an igloo within a time limit. The igloo is built piece-by-piece as the agent jumps on ice floes in water. The challenge is that the ice floes are in constant motion (moving either left or right), and ice floes only contribute to the construction of the igloo if they are visited in an active state (white rather than blue). The agent may also earn extra points by gathering fish while avoiding a number of fatal hazards (falling in the water, snow geese, polar bears, etc.). Success in this game requires a temporally extended plan to ensure the agent can accomplish a sub-goal (such as reaching an icefloe) and then safely proceed to the next sub-goal (see also Lake et al. (2017)). Ultimately, once all of the pieces of the igloo are in place, the agent must proceed to the igloo to complete the level before time expires. Our hypothesis for the better performance when using retrieval augmentation is that the retrieval process is able to efficiently utilize information from states that are far from the current state (i.e., it can perform temporally extended credit assignment). This hypothesis is further validated when we decrease the length of the traces in the dataset in our ablations. Decreasing the length of the retrieved and summarized trajectories reduces the amount of past and future information the retrieval process can retrieve. By default, the trajectories in the retrieval dataset are of length 80. To perform this ablation, we decrease the length of the effective context to only include information from 5 time-steps. When we perform this ablation, we see a significant decrease in performance on Frostbite.

A.3.6. AUXILIARY LOSSES IMPLEMENTATION.

Action, Value, and Reward Prediction. For training the representation used to summarize the trajectories in the retrieval batch, we use action, value and reward prediction as used in MuZero (Schrittwieser et al., 2020). We use the same loss

coefficient's and same architecture as proposed in MuZero (Schrittwieser et al., 2020).

BERT style losses. For self-supervised losses, we use a self-supervised vision representation similar to BERT developed in the natural language processing area. We use a masked sequence modeling task to train Transformers. Specifically, each trajectory has two views in our training, i.e, representation of each time-step, and visual tokens (i.e., discrete tokens). We first "tokenize" the representation of different time-steps into visual tokens. Then we randomly mask some visual tokens and fed them into the backbone Transformer. The objective is to recover the original visual tokens based on the corrupted tokens.

A.4. Gridroboman environment

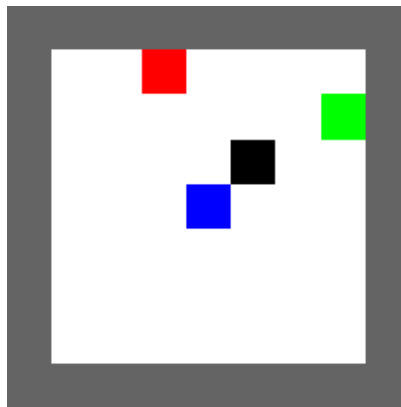


Figure 8: **Gridroboman environment illustration.** On the board there are three colored objects and the robot is represented by a black block. The robot can move itself and move the objects. The tasks are motivated by the robotic manipulation.

In order to test our method in a multi-task setting we designed a minimalistic grid world robotic manipulation (**gridroboman**) environment with a single embodiment and multiple tasks. It is implemented based on the `pycolab` (Stepleton et al.) game engine that provides tools for designing customizable grid world games. The environment and its tasks are inspired by the challenges in robotic manipulation. An illustration of a state in the environment is shown in Figure 3.

Environment semantics, observations and actions There are three colored objects on the 7×7 board: red, green and blue. The black block represents the robot. It can *move* in 4 directions and the action is skipped if it attempts to move into a wall (gray). Additionally, if the robot is located at the same position as any colored object, it can apply *lift* action that would enforce the object to move together with the robot. Then, *put* action allows to position the object either on the board or on the top of another single object. Additionally, there is an option of skipping an action. The initial state of the environment that includes positions of the objects and the robot is sampled randomly at the beginning of each episode. The agent observation is an 11-dimensional vector: it includes x and y coordinates of three objects and the robot as well as status of each of three objects. The status of an object is a numerical value: 0 if the object is positioned on the board, -1 if it is under another object and $+1$ if it is either held by the robot or located on the top of another object. Each episode lasts for 50 timesteps.

Tasks There are 30 possible tasks: lift red, green, or blue object (3), touch red, green, or blue object (3), move red, green, or blue to center (3) or to corner (3), touch one object with another (6), move two objects close to (3) or far from (3) each other, stack one object on the top of another (6). The nature of these tasks is such that it is impossible to identify the task by the initial state.

Rewards The reward is binary in each time step: it is zero when the task is not solved and one otherwise. In order to receive positive reward the following condition should be met:

- **lift X**: the robot should lift and not put back an object of color X;
- **touch X**: the robot should be located at the immediately adjacent cell to the object of X color and not hold any objects;
- **move X to center**: the object or color X should be located in the 3×3 block at the center of the board;
- **move X to corner**: the object of X color should be located in any of the 2×2 corners of the board;
- **touch X with Y**: the robot should be located at the immediately adjacent position to the object of X color and hold the object of color Y;
- **move X close to Y**: the distance between the objects of colors X and Y should be no more than 1 in both x and y direction;

- **move X far from Y**: the sum of distances between objects of colors X and Y in x and y coordinated should be greater than 9;
- **stack X on Y**: the objects of colors X and Y should be located at the same position one on the top of another.

A.4.1. GRIDROBOMAN EXPERIMENT SETUP

The gridroboman offline RL dataset was generated by training a single DQN agent online on each task separately and recording the 100K generated episodes. The $Q(s, a)$ network was a 3-layer MLP with 256 units in each hidden layer for Q-function. For the experiments with 10, 20, and 30 tasks, we use the first 10, 20, and 30 tasks, as listed here.

10 tasks: touch red, touch green, touch blue, lift red, lift green, lift blue, red touch green, green touch red, and green touch blue.

20 tasks: The above 10 tasks, blue touch red, blue touch green, red to corner, green to corner, blue to corner, red to center, green to center, blue to center, red close to blue, and red close to green.

30 tasks: The above 20 tasks, blue close to green, red far from blue, red far from green, blue far from green, red on blue, red on green, green on red, green on blue, blue on red, and blue on green.

A.4.2. GRIDROBOMAN HYPERPARAMETERS

The DQN agent used the same network as used to create the data: a 3-layer MLP with 256 hidden units per layer. The first 2 layers define f_{θ}^{enc} and the final layer predicts Q. The RA-DQN agent used the same base network plus a separate retrieval network.

Below we detail hyperparameters specific to gridroboman. Hyperparameters not specified in this section are the same as used in Atari.

- At each learner step, the agent samples a batch of 256 states from the replay buffer to train the DQN agent and further samples a batch of 64 trajectories from the retrieval dataset to form the retrieval batch.
- The retrieval process selects the top- $k_{\text{traj}} = 10$ trajectories with the highest return, and then retrieves relevant information from the selected trajectories (step 3, section 2.3) using the top- $k_{\text{states}} = 10$ most relevant states.
- To summarize the experiences in the retrieval batch we use a forward and backward GRU with 256 hidden units.
- We use 4 slots to parameterize the retrieval process.
- We use auxiliary losses in the form of value, reward, and policy prediction (section 2.2). We follow the same setup as proposed in (Schrittwieser et al., 2020) and weight these auxiliary losses with a coefficient of 0.1.
- The value of the β coefficient for the information bottleneck regularizer is fixed to 0.3.
- The hyperparameters and setup for offline DQN are taken from Gulcehre et al. (2020a). They are detailed in table 5. As in the above, we used double DQN (Van Hasselt et al., 2016).

Hyperparameter	Value
Optimizer	Adam
Learning rate	3e-4
Discount factor	0.99
Importance sampling exponent	0.2
Minimum sequences to start replay	5000
TD loss function	Huber(1.0)
Target Q-network update period	2500
Evaluation ϵ	6.5e-4

Table 5: Hyperparameters used in the gridroboman DQN experiments.

A.4.3. GRIDROBOMAN EVALUATION CURVES WHEN TRAINING ON ALL 30 TASKS

Figure 9 we show the average episode reward obtained by the evaluation agent on each individual task when training on all 30 tasks. Curves are shown for the DQN and RA-DQN agents.

A.5. BabyAI environment.

Observations, actions. We use the same setup for the observations and actions as in (Chevalier-Boisvert et al., 2018).

Tasks. We use all the 40 available tasks in the BabyAI environment.⁵

Hyper-parameters and RL algorithm. We follow the same setup as in the Gridroboman experiments. Since BabyAI is a partially observable environment, we summarize the history of the agent using a recurrent encoder.

Hyperparameter	Value
Optimizer	Adam
Learning rate	3e-4
Discount factor	0.99
Importance sampling exponent	0.2
TD loss function	Huber(1.0)
Target Q-network update period	1000
GRU hidden state	512

Table 6: Hyper-parameters used in the BabyAI Recurrent DQN experiments.

Retrieval Process. We use the same hyper-parameters for the retrieval process as used in the grid-roboman environment. For the case of multi-task retrieval buffer, we use 32 trajectories corresponding to each task to form the retrieval batch.

Analysis about retrieved information in the multi-task setting. We did some analysis to study the properties about the retrieved information in the multi-task setting in BabyAI. BabyAI setup contains about 40 tasks. Out of these 40 tasks, around 15 tasks are compositional i.e., requires to compose information from 2 or more sub-tasks, and rest of the tasks requires the agent to execute a particular behaviour (ex. going to the door, fetching a key etc). We study as to how often the agent retrieves information from other tasks. Ideally, for the compositional tasks, the hope would be the agent access information about the other tasks more often as compared to the tasks which require only a particular behaviour. So, during test time, we study the percentage of times agent access information from the same task as compared to accessing information from the different tasks. For compositional tasks, the agent access information from other tasks about 54% of times, while the percentage for single tasks is about 21%. That said, we were not able to find any pattern as to find why the agent is retrieving more information from other tasks for some particular tasks as well as any structure about the states from which information is being retrieved.

A.6. CausalWorld environment.

Observations, actions. We use the same setup for the visual observations and actions as in (Ahmed et al., 2020).

Tasks. We use 5 (out of 8 available tasks) in the CausalWorld environment (Ahmed et al., 2020) namely: Pushing, Picking, Pick and Place, Stacking2, Stacked Blocks.

Hyper-parameters and BC algorithm. For the retrieval augmentation, we follow the same setup as in the BabyAI and GridRoboman experiments. Due to its simplicity and strength as a baseline (Gulcehre et al., 2020b), we use behavior cloning as the underlying algorithm.

⁵https://github.com/mila-iqua/babyai/blob/master/docs/bonus_levels.md. https://github.com/mila-iqua/babyai/blob/master/docs/iclr19_levels.md

Retrieval Augmented Reinforcement Learning

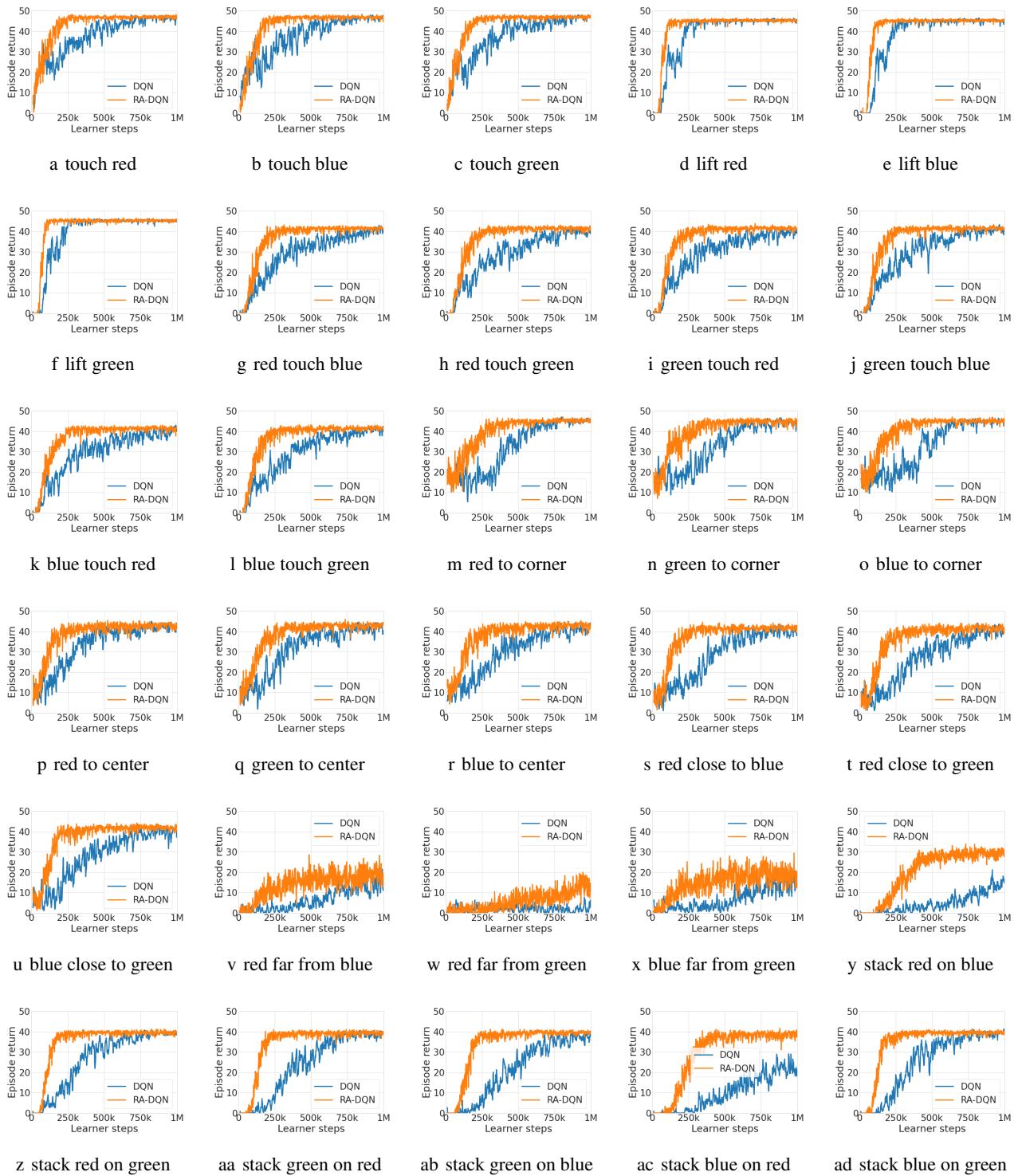


Figure 9: **Multi-task offline RL with a task-specific retrieval dataset.** Evaluation performance for RA-DQN (orange) and baseline DQN (blue) when training on all 30 gridworld tasks with a single agent. Curves show the performance of each agent (averaged over 3 seeds) when running that agent online in the environment on the specified task.